

**APPLICATION OF FLOWBACK WATER AND GOPS AND GOPS ON THE
PREVENTION OF ACID MINE DRAINAGE IN THE MATHER MINE**

by

Huiqi Deng

B.S. in Environmental Engineering, Sun Yat – Sen University, China 2011

Submitted to the Graduate Faculty of
Swanson School of Engineering in partial fulfillment
of the requirements for the degree of
Master of Science

University of Pittsburgh

2013

UNIVERSITY OF PITTSBURGH
SWANSON SCHOOL OF ENGINEERING

This thesis is presented

by

Huiqi Deng

It was defended on

July 17, 2013

and approved by

Leonard W. Casson, PhD, Associate Professor, Department of Civil and Environmental
Engineering

Anthony T. Iannacchione, PhD, Associate Professor, Department of Civil and Environmental
Engineering

John C. Brigham, PhD, Assistant Professor, Department of Civil and Environmental Engineering

Thesis Advisor: Leonard W. Casson, PhD, Associate Professor, Department of Civil and
Environmental Engineering

Copyright © by Huiqi Deng

2013

**APPLICATION OF FLOWBACK WATER FROM GAS DRILLING AND GOPS ON
THE PREVENTION OF ACID MINE DRAINAGE IN MATHER MINE**

Huiqi Deng, M.S.

University of Pittsburgh, 2013

Acid mine drainage (AMD) is an environmental pollutant that degrades water bodies and harms aquatic life. In the Appalachian Mountains of the eastern U.S., over 7,500 miles of streams are impacted by AMD. Current methods of active treating AMD such as neutralization with limestone are labor-intensive and costly. Passive treatments with lower maintenance and management costs are the more sustainable alternatives for AMD management. The research reported herein explores the possibility of applying flowback water from natural gas drilling operations and the chelating agent 3-glycidoxypropyltrimethoxysilane (GOPS) as additive to passively treat AMD. The hypothesis is that chemicals present in the flowback water will form insoluble salts with those in the mine residue and precipitate on the mine rock to passivate the surface.. Additionally, GOPS will improve upon the passivation process by complexing with metal ions in the precipitate to form a multilayer hydrophobic coating.

In order to develop a protocol for measuring the optimal dosage of flowback water and GOPS for AMD prevention, several preliminary batch tests were conducted. These tests evaluated the reaction time and volumes of flowback water and GOPS appropriate for further column testing, as measured by concentrations of Fe, Ba, and SO_4^{2-} . From batch studies, it is

observed that when 55 mL of flowback water was added to 500 mg of mine residue, the contaminants of major concern, Fe and SO_4^{2-} reached their lowest levels. Meanwhile, a dosage of 0.0001 M GOPS is optimum to improve the microencapsulation. Results from the test column were compared to an identical control column, which was treated with deionized water. The results suggest that, for the experiment duration of one month, flowback water and GOPS have done an effective job in curbing the release of Fe and SO_4^{2-} from mine residue. After 15 days of treatment, the concentration of Fe was 0.6 ppm, reduced by 96% relative to the control, and the concentration of SO_4^{2-} was 90 ppm, reduced by 83%. However, trace metals including Mn were not reduced to within the requirements set by the Environment Protection Agency. As a result, more studies are needed to improve the performance of this technique.

TABLE OF CONTENT

ACKNOWLEDGEMENTS	xii
1.0 INTRODUCTION: ACID MINE DRAINAGE.....	1
1.1 ENVIRONMENTAL CONSEQUENCES OF ACID MINE DRAINAGE	1
1.2 OBJECTIVE	3
2.0 BACKGROUND	5
2.1 ACID MINE DRAINAGE FORMATION	5
2.2 ACID MINE DRAINAGE TREATMENT.....	10
2.2.1 Active Treatment of Acid Mine Drainage	10
2.2.2 Passive Treatment of Acid Mine Drainage.....	13
2.3 ACID MINE DRAINAG SOURCE AND CONTROL	14
2.4 ALTERNATIVE – MICROENCAPSULATION (COATING).....	15
2.4.1 Mechanisms.....	16
2.4.2 Prior Study of the Prevention of Pyrite Oxidation Through Microencapsulation	18
2.4.2.1 Iron (oxy)hydroxide ($\text{Fe}(\text{OH})_3/\text{FeOOH}$) coating.....	19
2.4.2.2 Pyrite Passivation by Phosphate.....	21
2.4.2.3 Pyrite Passivation by Phospholipid.....	23
2.4.2.4 Pyrite Passivation with Silicate.....	23
2.4.3 Summary	27

3.0 MATERIALS AND METHODS	29
3.1 INTRODUCTION	29
3.2 MATERIAL AND SAMPLE PREPARAION.....	30
3.2.1 Solutions and Other Chemicals	30
3.2.2 Source of Mine Waste and Flowback Water.....	30
3.2.3 Preparation of Mine Waste and Flowback Water.....	31
3.3 EXPERIMENTAL PROCEDURES.....	32
3.3.1 Batch Studies	32
3.3.2 Volume of Flowback Water.....	33
3.3.3 Duration of Mixture Agitation	33
3.3.4 Effect of Hydrogen Peroxide.....	34
3.3.5 Effect of 3-glycidoxypropyltrimethoxysilane (GOPS, C ₉ H ₂₀ O ₅ Si).....	34
3.3.6 Effect of Hydrogen Peroxide and GOPS.....	35
3.3.7 Column Studies.....	35
3.4 SAMPLE ANALYSIS	37
4.0 RESULT AND DISCUSION.....	39
4.1 INTRODUCTION AND OBJECTIVE.....	39
4.2 BATCH STUDIES.....	39
4.2.1 Sieve Analysis	39
4.2.2 Selection of Ratio Between Fracturing Water and Mine Residue	42
4.2.3 Selection of Equilibration Time	46
4.2.4 Effect of H ₂ O ₂ in Suppression for Pyrite Oxidation	49
4.2.5 Effect of GOPS on Suppression of Pyrite Oxidation	54
4.3 CONTINUOUS COLUMN STUDIES	63
4.3.1 pH	64

4.3.2 Al	65
4.3.3 Fe	67
4.3.4 Sulfate	70
4.3.5 Mn.....	72
5.0 SUMMARY AND CONCLUSIONS	74
5.1 PRELIMINARY EXPERIMENTS.....	74
5.2 COLUMN EXPERIMENTS	76
6.0 FUTURE RESEARCH	78
6.1 SUGGESTIONS ON FURTHER RESEARCH ON THIS WORK.....	78
6.2 APPLICATIONS	79
BIBLIOGRAPHY	82

LIST OF TABLES

Table 1 Studies Conducted in This Thesis Program.....	29
Table 2 Composition of Mine Residue from The Mather Mine.....	31
Table 3 Particle Size Distribution of Mine Residue from Mather Mine.....	40
Table 4 pH of Flowback Water and Deionized Water vs. Volume of Fluid Added.....	44
Table 5 pH in Flowback Water and Deionized Water vs. Reaction Times	47
Table 6 [Fe] in Flowback Water and Deionized Water vs. Reaction Time.....	47
Table 7 [Ba] in Flowback Water and Deionized Water after Various Reaction Time	47
Table 8 Effect of Hydrogen Peroxide Treatment on pH.....	51

LIST OF FIGURES

Figure 1 Schematic of Proposed Microencapsulation Technology (Evangelou, 1996).....	22
Figure 2 Schematic of Ferric Oxides - Silica Coating (Karbgo et al. 2005).....	26
Figure 3 Schematic of Batch Apparatus	33
Figure 4 Schematic of Column Apparatus.....	37
Figure 5 Particle Size Distribution of Mine Residue from Mather Mine	41
Figure 6 Mass of Fe, Ba, and SO_4^{2-} Recovered vs. Volume Flowback Water Addeed.....	44
Figure 7 Fe Removal vs. Time.....	48
Figure 8 Ba Removal vs. Time	48
Figure 9 The interaction between H_2O_2 with Fe^{3+} and Fe^{2+} (Evangelou, 1995 (B))	50
Figure 10 The interaction between H_2O_2 on $[\text{Fe}]$	51
Figure 11 Effect of H_2O_2 Treatment on $[\text{Ba}]$	52
Figure 12 Structure of GOPS.....	55
Figure 13 Hydrolysis of GOPS (Schmidt, 1994).....	55
Figure 14 Effect of $[\text{GOP}]$ on pH	56
Figure 15 Effect of $[\text{GOP}]$ on Fe	57
Figure 16 Reaction of GOPS (Schmidt, 1985)	58
Figure 17 Crosslinking/Polymerization of GOPS (Schmidt 1985;1986)	59
Figure 18 General Polymerization of GOPS (Schmidt, 1994)	59
Figure 19 Crosslinking of GOPS with Fe Hydroxide and Al Hydroxide.....	61
Figure 20 Effect of GOPS Treatment on $[\text{Ba}]$	62

Figure 21 pH in Control Column & Test Column	64
Figure 22 Concentration of Al in Control Column & Test Column	65
Figure 23 Concentration of Fe in Control Column & Test Column	67
Figure 24 Concentration of Sulfate in Control Column & Test Column.....	70
Figure 25 Concentraion of Mn in Control Column & Test Column.....	72

ACKNOWLEDGEMENTS

I would like to acknowledge the following for their funding and support throughout my research:

- Dr. Leonard W. Casson
- Dr. Anthony T. Iannacchione
- Dr. John C. Brigham
- Dr. Jason Monnell
- Dr. Xu Liang
- My dear husband, Karl Debiec, who is always there for me, and my family, who offer me love unconditionally, and my friends, especially Bryanna Snyder, Mike Sweriduk, Megan Ponzio, and Fangling Ji.

1.0 INTRODUCTION: ACID MINE DRAINAGE

1.1 ENVIRONMENTAL CONSEQUENCES OF ACID MINE DRAINAGE

Excavations of natural resources, such as mining and ore operations as well as highway construction, may come at a severe price to the environment. The mining waste, ore tailings, and overburden resultant from mining activities may give rise to acidification of water bodies and destruction of living organisms. Acid mine drainage (AMD) is a term used to describe the acidic water resulting from mining activities and is regarded as a severe environmental pollutant, involving large sums of money for its prevention and treatment throughout the world every year. During active mining operations, there was historically little concern for the generation of AMD while the water tables were kept artificially low by pumping. However, when active mining operations cease and pumping stops, the water table rebounds and makes favorable conditions for producing AMD. It is reported that the problem of AMD can occur for hundreds of years after mines are closed and abandoned (Egiebor et al., 2007). Unfortunately, not until the latter half of the 20th century did efforts by industry to mine in a sustainable and environmentally neutral manner become widespread. High acidity and high concentrations of metals are two major characteristics of AMD. These leachates are responsible for the environmental deterioration of rivers, groundwater and soil. In addition, AMD is enriched with iron, aluminum, magnesium, sulfate and heavy metals such as lead and cadmium. The high mobility of dissolved

solids in the AMD can be explained by the fact that the metals tend to remain dissolved in water as ions under acidic pH rather than precipitating, which is more likely to happen under alkaline pH. The discharge of acidic and metal-enriched AMD is responsible for the poisoning of vegetation and contamination of the other water systems when rainfall and snowmelt flush this toxic solution downstream.

In the eastern United States, the streams and rivers that are contaminated with AMD are a total of approximately 20,000 km, 90% of which are caused by abandoned underground coal mines (U.S. Environmental Protection Agency (EPA), 1995). But since no company or individual claims responsibility for reclaiming abandoned mine lands, the treatment of the AMD origins or rivers has become a public issue and expense (Ziemkiewicz et al, 1997). Now, mining companies are required to meet the environmental land reclamation performance standards established by federal (the Surface Mining Control and Reclamation Act, SMCRA) and state regulations. Mining operators are also required to meet the water quality standards set in the Clean Water Act of 1972 (CWA). According to the CWA, each mining operation must acquire a National Pollutant Discharge Elimination System (NPDES) permit, in addition to a surface mining permit. The NPDES permits for surface mining require monitoring of pH, total suspended solids (TSS), and Fe and Mn concentrations (Skouson et al., 1998). In order to meet the discharge standards, substantial reagents, equipment, and labor are required for the substantial maintenance of treatment for AMD. Lovett and Ziemkiewicz (1991) estimated ammonia chemical costs for a site in West Virginia at \$72,000 per year and floc handling costs of \$486,000 per year. The problems caused by AMD are serious and costly. As a result, significant demands should be placed on preventing the formation of AMD at its source or treating AMD already formed in an economically feasible and long-lasting fashion.

1.2 OBJECTIVE

In this research study, the possibility of applying flowback water, the wastewater from shale gas fracturing, towards the treatment of acid mine drainage has been explored. To this end the following tests have been conducted:

- Determine if flowback water is able to successfully treat acid mine drainage, and if so determine the optimal ratio between mine waste and flowback water
- Determine if H₂O₂ is able to improve AMD treatment with flowback water, and if so determine the optimal ratio
- Determine if GOPS is able to improve AMD treatment with flowback water, and if so determine the optimal ratio
- Validate the treatment of AMD with flowback water in conditions close to real-world usage, in a continuous-flow column environment

The benefit of using flowback water for AMD prevention and treatment is that, through appropriate design, the chemistry occurring between mine residue and flowback water may make these two wastes neutral, reducing their adverse environmental impacts. Both the treatment of flowback water and AMD are costly and energy intensive. As a result, this suggested research may solve these both these severe environmental problems with less energy. The results observed in this research indicate an effective approach to prevent further AMD formation. Although some contaminants still fail to meet the regulations set by the EPA, this approach may

still serve as the first stage of AMD treatment, followed by other treatments to remove the rest of contaminants, such as coagulation, activated carbon, and microfiltration. Flowback water, once applied properly, may be a valuable resource rather than a waste that requires intensive treatment.

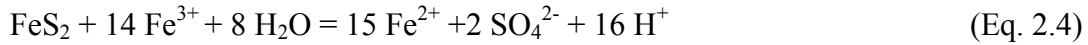
2.0 BACKGROUND

2.1 ACID MINE DRAINAGE FORMATION

Upon exposure to oxidizing environments and in the absence of alkaline materials (such as calcium carbonate as present in limestone), sulfide minerals that are commonly included in and surrounding coal are immediately susceptible to chemical and microbiological oxidation.

Pyrite (FeS_2) is the most important member of the disulfide group and is also the most abundant sulfide mineral in the earth's crust (Vaughan 1978). The common iron-sulfide minerals pyrite (FeS_2) and less common pyrrhotite (FeS) and marcasite (FeS_2) are the dominant sources of acidity in PA (Pennsylvania Department of Conservation and Natural Resources). Besides coalfields, pyrite is also ubiquitous in many ores. Pyrite oxidation takes place when pyrite-bearing minerals are exposed to oxygen and water. This process is complex for it involves chemical and microbiological reactions, and it varies with geological conditions. Factors like pH, oxygen concentration, pyrite morphology and reactive surface area, catalytic agents (bacteria), and in-situ hydrology have been found to influence or even determine the rate of pyrite oxidation (Evangelou, 1995). As a result, AMD composition may vary considerably from mine to mine. It is possible for some mine effluents to exceed the regulatory standards for metals and acidity by several orders of magnitude even as others are within regulation (Egiebor et al., 2007).

From the chemistry standpoint, the oxidation of FeS₂ and subsequent reactions are shown in **Equations 2.1-2.4** (Singer & Stumm et al., 1970).



These equations combine to form a rapid cycle for the production of AMD, which is typically associated with the release of a large amount of acids and metals. The pyrite oxidation cycle is initiated by exposing pyrite to atmospheric oxygen and water, producing ferrous iron (Fe²⁺, the reduced form of iron), sulfate (SO₄²⁻), and acid. The ferrous iron originating from the first step is oxidized further by the oxygen to form ferric iron (Fe³⁺, the oxidized form of iron). The conversion from Fe²⁺ to Fe³⁺ under abiotic conditions is concluded by Stumm and Morgan (W. S. et al., 1981) to be the rate-limiting step in the oxidation of pyrite with a half-life of more than 100 days. Accordingly, it is known that the availability of oxygen is the limiting factor in this process. When the pH is above 3.5, Fe³⁺ precipitates as amorphous iron hydroxide (Fe(OH)₃) and releases additional protons as a product of hydrolysis (Nordstrom, 1982). This initial stage of pyrite oxidation is a slow process, with a dissolution rate of pyrite at about 6.2 × 10⁻¹⁰ mol m⁻² s⁻¹ at pH 7 (Lapakko & Antonson, 2006). Singer and Stumm suggested a fourth-order relationship with pH, indicating that hydrolysis reaction shifts from a very rapid rate at pH >3 to a very slow rate at pH <2.5 (Hedin et al., 1993). It should be kept in mind that the pH of freshly exposed pyritic materials is usually above four, thus dissolved oxygen is the main oxidant and the rate of oxidation is still relatively slow in the beginning of pyrite oxidation (Huminicki et al., 2009). Nevertheless, with the release of acidity shown in **Equation 2.3**, the pH in solution as

well as the pyrite surface pH drop continuously. When the pH is below 3.5, the pyrite acts as a powerful oxidant to oxidize Fe^{2+} and produce acidity. In fact, compared with oxygen, Fe^{3+} is a stronger oxidant for pyrite oxidation and it has been established as the primary oxidizing agent for the pyrite oxidation process (Perez-Lopez et al., 2007). Additionally, it has been noted that at low pH (<4.5), pyrite is oxidized by Fe^{3+} much more rapidly than that by atmospheric oxygen (Singer & Stumm, 1970). Moses et al. (1991) reported that even at neutral pH, Fe^{3+} is still an effective pyrite oxidant. As long as the dissolved Fe^{3+} is present, pyrite may be attacked by Fe^{3+} and pyrite oxidation may continue. In other words, the oxidation of pyrite by dissolved Fe^{3+} becomes the main mechanism for the formation of AMD at pH below 3.5 ((Singer & Stumm, 1970; Moses et al. 1987).

As can be seen in **Equations 2.1-2.4**, it is sulfur that is oxidized in the cycle, but not iron, since it is Fe^{2+} initially in the pyrite and it remains Fe^{2+} in the effluent. From a hydrogeological point of view, mine tailing or overburden can be characterized as highly porous and unsaturated (Collin et al., 1987). This means that even when the atmospheric oxygen is depleted by the initial oxidation, the oxygen can be quickly replenished due to the presence of oxygen in the atmosphere. Further, as discussed previously and indicated in **Equation 2.4**, in the absence of oxygen, Fe^{3+} (the stronger oxidant) can carry on reacting with pyrite and complete the oxidation cycle.

It is evident that the oxidation process of pyrite is accompanied by a significant production of protons (for every mole of pyrite, four moles of protons are actually produced), explaining the high acidity in the leachates. Unfortunately, under conditions of limited alkalinity, no natural neutralization occurs and water quality degradation results. This oxidation cycle is further complicated by the fact that pyrite is a semiconductor (Lalvani et al.,1996). The electrons

are transferred from sulfur atoms at anodic sites, attracting oxygen atoms in water molecules to form sulfoxy species via electromagnetism (Rimistidt & Vaughan, 2003). These chemical reactions are electrochemical in nature, meaning that pyrite is rather reactive and various reactions can happen in various sites of the pyrite (Rimistidt & Vaughan, 2003).

When the pH is less than 4, abiotic Fe oxidation becomes a less important mechanism for pyrite oxidation, because the oxidation cycle is greatly accelerated by acidophilic iron-oxidizing bacteria, especially *T. ferrooxidans* (Jaynes et al. 1984). In this range of pH (<4), the microorganisms, mainly iron oxidizing bacteria catalyze the oxidation of Fe^{2+} to Fe^{3+} by six orders of magnitude (Singer & Stumm, 1970). *T. ferrooxidans* is an acidophilic/chemolithotrophic organism that is universally present in geological strata associated with pyrite (Nordstrom 1982). Thereby, the elimination of iron-oxidizing bacteria in the vicinity of pyrite surface at acidic pH is necessary for the prevention of pyrite oxidation. At neutral to alkaline pH, the concentration of Fe^{3+} decreases dramatically due to the combined effects of precipitation of ferric hydroxides and the diminished activities of the acidophilic iron-oxidizing bacteria (Evangelou, 1995 (a)). This suggests that the elevation of pH plays a vital role in hindering the pyrite oxidation catalyzed by acidophilic iron-oxidizing bacteria at acidic pH. But at the same time, when the pH is one unit higher, the abiotic conversion rate from Fe^{2+} to Fe^{3+} is 100 times faster (Singer & Stumm, 1970). It was determined by Silverman in 1967 that *T. ferrooxidans* and *F. ferrooxidans* are strictly aerobic and the oxygen is the only electron acceptor that sustains the bacterial oxidation of Fe^{2+} to Fe^{3+} iron. This implies that exclusion of oxygen from pyrite surface can aid in getting rid of the oxidizing bacteria in this complicated process. In summary, pH neutralization and dissolved oxygen exclusion are two approaches that can be counted on to eliminate iron-oxidizing bacteria around pyrite surface.

The reactivity of pyrite is also influenced by its specific surface area available for the reactions to take place. It has been pointed out by some researchers that pyrite oxidation is a surface controlled reaction (Hoffmann et al. 1981). Naturally, framboid/polyframboid pyrite with high specific surface area and high porosity is reported to account for more than 50% of pyrite in underground coal mining (Caruccio et al. 1977; Evangelou et al. (b) 1995). The fast oxidation rate of pyrite may also be attributed to its massive surface area for environmental and microbiological contact.

The chemistry of AMD is heavily influenced by acid-producing (sulfide) and acid-neutralizing (carbonate from limestone in geological strata) minerals around the mine rock surface (Skousen et al. 2002). Acid base counting is a well established tool for predicting whether there is sufficient alkalinity generating material in pyrite containing minerals. Acidity in this case is composed of “proton acidity” and “mineral acidity” (the combined concentration of dissolved metals, releasing proton during hydrolysis). In eastern United States, the acidity is usually comprised of pH, Fe, Al and Mn (Hedin et al. 1991).

$$\textit{Estimated Acidity} = 50 \left(2 \frac{\textit{Fe}^{2+}}{56} + 3 \frac{\textit{Fe}^{3+}}{56} + 3 \frac{\textit{Al}^{3+}}{27} + 2 \frac{\textit{Mn}^{2+}}{55} + 1000 (10^{-\textit{pH}}) \right) \quad (\text{Eq. 2.5})$$

Limestone is a natural source to offer alkalinity and offset acidity. Limestone (CaCO_3) can dissolve in solution and release carbonate (CO_3^{2-}) and bicarbonate (HCO_3^-), which are well known as buffers that curb the drastic pH fluctuation by reacting with protons. Generally, sites with rich carbonate and small amount of sulfide tend to produce alkaline or neutral water, as opposed to sites with rich sulfide and poor carbonate, where AMD is generated. In some cases, the pH of AMD can be as low as 2.

2.2 ACID MINE DRAINAGE TREATMENT

The acidic effluent already formed is the symptom of AMD while the pyrite oxidation is the source. Numerous prior investigations have been undertaken to seek techniques to remedy the AMD problem. Some researchers directed efforts towards the treatment of its symptom, others aim to suppress its origin: the pyrite oxidation process. Both chemical and biological treatment systems can be divided into two categories: active treatments (requiring substantial input of chemicals and maintenance to perpetuate an effective treatment) and passive treatments (requiring relatively less input of other resources after set up). Although the mitigation of AMD has been intensively studied, a scientifically sound and economically feasible passive technique has not been identified.

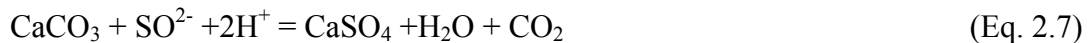
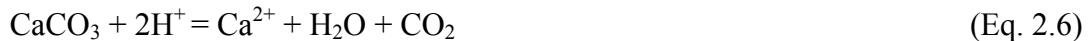
2.2.1 Active Treatment of Acid Mine Drainage

Active treatments allow the formation of AMD to run its course and treat the resultant symptoms afterwards. The widespread strategies used in active treatment are to raise the pH in solution with addition of alkaline chemicals, accelerating the production of Fe^{3+} . This artificial alkaline addition and increase in pH leads metals to precipitate as hydroxides and carbonates. Ideally, the rate of addition of alkaline materials should exceed the rate of generation of acidity emanating from the pyrite oxidation. The neutralizing chemicals applied include: calcium carbonate, lime, slaked lime, caustic soda, and soda ash. However, the techniques of active treatment usually have

a short life span and require a long-term commitment to site management. This means that they require regular equipment maintenance, manpower, and pumping, which can be rather costly and impractical for the treatment of AMD in remote and abandoned mines (Ziemkiewicz et al. 2007).

Additionally, the bulky sludge that results as the metals are removed as solids from solution needs to be disposed of. In some cases, flocculating reagents, which are conducive to their aggregation are used to enhance their removal in settling ponds (Johnson et al. 2005). Sometimes, aeration is used to aid the oxygenation of ferrous iron.

Limestone, being an inexpensive and available alkaline material, is the widely used in the treatment of AMD. However, it is inevitable that gypsum (**Equation 2.6**) and ferric (oxy)hydroxides form and block the limestone surface, eliminating any further neutralizing capability (Egiebor et al. 2007; Wentzler et al. 1992). The reactions concerning limestone neutralization are (Wentzler et al. 1992):



Theoretically, attempts to abate or treat AMD through addition of alkaline materials containing carbonate are prone to be ineffective. Because of the high affinity of Fe^{3+} to OH^- , soluble ferric hydroxides are present as $\text{Fe}(\text{OH})^{2+}$, $\text{Fe}(\text{OH})_2^+$, $\text{Fe}(\text{OH})_3$, and $\text{Fe}(\text{OH})_4^-$. Interestingly, due to the fact that the surface of pyrite is negatively charged, $\text{Fe}(\text{OH})^{2+}$ and $\text{Fe}(\text{OH})_2^+$ can be absorbed to the surface of pyrite due to the electrostatic force. At neutral or alkaline pH, the predominant form of carbonate from limestone is HCO_3^- . Consequently, there is a great potential for HCO_3^- to react with surface Fe^{2+} -S-S: $\text{Fe}_2(\text{OH})^+$ and form a Fe^{2+} -S-S: Fe_2CO_3 complex, accelerating Fe^{2+} oxidation (Evangelou, 2001). This means that more Fe^{3+} is produced to promote the oxidation cycle. This is consistent with the observation that the rate of the

neutralization reaction decreases notably with increasing pH and limestone is stated to be ineffective above pH of 5 (Egiebor et al. 2007).

Numerous studies have been carried out to look for substitute alkaline materials. These researches studied the use of zeolite (Golab et al. 2006), red mud (McConchie et al. 2002), forsterite (Kleiv et al. 2001), and caustic magnesia (Cortina et al. 2003). However, none of these shows great advantage over traditional alkaline materials when it comes to treatment effectiveness and cost.

Recently, coal combustion by-products, mainly fly ash, have been investigated as the acidity-consuming material to precipitate metals. Fly ash tends to cement the mineral surface and form a hardpan on the top after wetting (Perez-Lopez et al. 2009). It is documented that the layer of cement on the top acts as a strong physical barrier to exclude water and oxygen from contacting the mine refuse. Similarly, waste material with significant neutralization potential (NP), like scrubber sludges from power generation, kiln dust and steel slags, can also raise pH and form a cement on the top. It is true that these combustion by-products did a good job in reducing acidity and immobilizing metals. However, they have the disadvantage that various heavy metals such as arsenic and selenium are accumulated in them during processing and migrate to mine refuse and the environment during their utilization. For instance, mercury is abundant in fly ash and it has potential mobility to disposal environments when fly ash is used in AMD treatment (M.A. B. et al. 2007).

2.2.2 Passive Treatment of Acid Mine Drainage

In order to avoid the armoring of limestone due to precipitation, anoxic limestone drains (ALDs) have been used as a passive treatment. Plastic, clay, or soil linings have been employed in ALDs to impede the penetration of oxygen and to curb the conversion of Fe^{2+} to Fe^{3+} . However, incomplete contaminant removal in the effluent has been reported by some researchers (Egiebor & Oni, 2007; Johnson et al. 2005). Just as with alkaline addition, appropriate sludge disposal imposes additional maintenance and expense for the treatment system.

Rather than counting on chemical approaches, natural/constructed wetlands have also been determined to be useful in ameliorating AMD as it passes through the wetlands, which is low in cost and maintenance requirement. These wetlands are chiefly composed of plants that prefer slightly acidic to moderately acidic environments. Meanwhile, these plants show high tolerance to high concentrations of metals and sulfate that are dangerous to most of other plants (Hedin et al. 1993). The mechanisms that play a pivotal part in wetlands involve adsorption, ion exchange, bioaccumulation, bacterial and abiotic oxidation, sedimentation, neutralization, and sulfate reduction (Wildeman et al. 1993). Two types of wetlands, aerobic wetland and anaerobic wetland, predominate the engineered wetlands landscape. Because of the shallow water surface, and low flow rate, aerobic wetlands are beneficial for metal oxidation and hydrolysis. Thereby, aerobic wetlands tend to retain metals like Fe, Al and Mn as precipitates. In anaerobic wetlands, sulfate reduction takes place as the reverse reaction of pyrite oxidation, consuming acidity. In this process, sulfate-reducing bacteria, known as heterotrophic anaerobic bacteria, decompose organic compounds using sulfate as the electron acceptor and produce hydrogen sulfide, which reacts with other metals in solution to produce sulfide compounds (Kleinmann & Hedin, 1989). ALDs are also used to pretreat AMD to lower the acidity that the following wetlands would

receive and markedly reduce the size demands for wetland to accomplish certain removal standards (Hedin et al. 1993).

2.3 ACID MINE DRAINAG SOURCE AND CONTROL

It has been demonstrated that oxygen, water, and iron-oxidizing bacteria are three components responsible for the formation of AMD. As a consequence, some at-source control and prevention of AMD techniques have been proposed in an effort to eliminate one or more elements in this pyrite oxidation cycle and slow the onset of AMD formation.

Anionic surfactants such as triethylenetertramine (TETA), diethylenetriamine (DETA) and sodium lauryl sulfate (SLS) are suggested as bactericides to eliminate the significant catalyzing effect brought out by iron-oxidizing bacteria. They are often sprayed by trucks on cells of residue in backfill or used in the refuse conveyor belts (Parisi et al 1994). However, the application of these bactericides may fail eventually as the surfactants leach out of the rock or are decomposed. Moreover, although the bacterial activity of oxidation has been controlled, abiotic oxidation continues. Plus, the presence of the bactericide in effluent may impose severe effects on aquatic organisms. Thus, the application of bactericide is not a feasible solution.

Flooding or sealing of underground mines has been explored as an alternative to limit the ingress of dissolved oxygen in water. Oxygen initially present in water would be consumed by microorganisms living in flooding water and its replenishment is difficult due to the negligible exchange with the atmosphere. But this approach is only practical for sites of specific design (Johnson et al. 2005).

Other approaches make use of low-permeability materials such as polyethylene and asphalt to cover the waste material and vegetation to reduce the infiltration of water and ingress of air. However, these techniques are only successful temporarily in as much as the pyrite oxidation is only triggered by an extremely low partial pressure (of the order of 10^{-30}) and it is unfeasible to prevent the water infiltration into the highly porous minerals in mining environments (S.C. & R. Z. 1992).

2.4 ALTERNATIVE – MICROENCAPSULATION (COATING)

Preventing a problem in the first place is preferable to treating it after it already existst. The inhibition of pyrite oxidation and control of AMD at its source is the permanent and most promising solution to the AMD problem. Recall that pyrite oxidation is initiated with atmospheric oxygen to produce protons, sulfate and Fe^{2+} , but continues without and depends on Fe^{3+} . With the release of protons, the pH decreases to below 3.5, where the reactivity of Fe^{3+} increases dramatically and serves as the principal oxidant for acid production. Under acidic environments, iron-oxidizing bacteria, especially *T. ferrooxidans*, catalyze the oxidation of Fe^{2+} to Fe^{3+} . According to the discussion above, pyrite oxidation can be remarkably attenuated through reducing the reactivity of Fe^{3+} ., the powerful and major oxidant in this case, depleting the atmospheric oxygen available, and inputting alkaline material to prevent the pH from dropping below 3.5 and to promote the precipitation of ferric (oxy)hydroxide. Any attempts including those listed above would be reliable to curb the pyrite oxidation. The key to preventing AMD is to prevent Fe^{3+} and/or O_2 from contacting the pyrite surface. The technique of microencapsulation aims to build a physical barrier to impede the electron transfer between

oxidants and the pyrite surface, and to reduce the activity of Fe^{3+} through formation of complexes or precipitates. The coating used for microencapsulation may be either inorganic or organic in origin.

2.4.1 Mechanisms

Microencapsulation makes use of coating deposition to inactivate the surface reactivity. Fe^{2+} is first oxidized to Fe^{3+} , which may in turn react with the incorporated chemicals to precipitate as layer(s) of coating on the pyrite surface. This technology is different from complexation, which reduces the concentration of active Fe^{3+} in solution and thus, its oxidation potential. EDTA and DTPA are two reagents which are capable of strongly complexing with Fe^{3+} . They have been used in the inhibition of pyrite oxidation by Huang and Evangelou (1994) and Brown and Juriank (1989) respectively. The field emission microscope (FEM) images in their investigation show that after leaching pyrite with EDTA and DTPA, the pyrite surface is free of coating and the its oxidation is intact. In other cases, some organic reagents, such as humic acid and other chemicals leached from manure or wood chips, may also be used as complexation agents. However their effectiveness under acidic pH is questionable (Lalvin et al. 1996). However, complexation is not intended to coat and inactivate the grain surface, and therefore in the long run is less effective than microencapsulation.

A successful microencapsulation implementation is accomplished through introducing treatment chemicals, which are intended to strongly complex with Fe^{3+} and form a stable and robust coating on the mineral surface. The complex should be insoluble under acidic environments as well. In some cases, hydrophobic tails can also be introduced to the complex to

interrupt the contact between mineral surface and water, which is a key element in the oxidation cycle.

At alkaline pH, pyrite oxidation takes place rapidly and the Fe^{3+} released from pyrite was immediately consumed as Fe (oxy)hydroxide and its complexes that deposit on the mine residue surface. With time, these deposits grow thicker and denser. As discussed above, the bacteria that catalyze the oxidation of Fe^{2+} to Fe^{3+} are acidophilic. Under alkaline conditions, their catalytic role would be suppressed. As the initial release of Fe^{3+} contributes to building a barrier around the mine residue surface, its oxidation potential would diminish. By doing so, the principal oxidant in the pyrite oxidation cycle has been controlled. In view that oxygen is the limiting fact of the oxidation process, the coating, exerted by ferric (oxy)hydroxide and its insoluble complexes, would do a great job in inhibiting the diffusion and transport of oxygen, and thus block the interaction between the other oxidants and the pyrite. As a consequence, theoretically, microencapsulation with ferric (oxy)hydroxide and its complexes shows great prospect in passivating mine residue surface and solving the AMD problem at its source.

The pyrite surface is described by a model of piles, which is partially and randomly covered with three-dimensional heterogeneous oxidized phases, containing five main species: (1) highly hydrated ferric sulfate $\text{Fe}_2(\text{SO}_4)_3 \cdot n\text{H}_2\text{O}$ ($n \approx 9$), (2) less hydrated ferric sulfate species $\text{Fe}_2(\text{SO}_4)_3 \cdot n\text{H}_2\text{O}$ ($n = 0-7.5$), (3) ferric hydroxide $\text{Fe}(\text{OH})_3$ or oxyhydroxide FeOOH , (4) ferrous hydrated sulfate $\text{FeSO}_4 \cdot n\text{H}_2\text{O}$, where n is from 0 to 7, (5) polysulfate FeS_5 and (6) elemental sulfur S_8 . Hydrated iron species are mainly located at the top of piles, with iron hydroxide ($\text{Fe}(\text{OH})_3$) and oxide (FeOOH) inside and sulfur species at the bottom. All species are in equilibrium with each other depending on environmental variables, such as concentration and pH. Oxide iron species and elemental sulfur are quite stable in water solution because of their

low solubility and highly hydrophobic character, respectively. From a chemical point of view, species 2, 3, and 4 can be considered as potential chemical adsorption sites. The Fe^{3+} species 2 and 3 were reported to have strong affinity to organic molecules. The points mentioned above are the basis for adsorption on pyrite surface in dynamic conditions (J.R., C et al. 1998). When pyrite oxidation releases Fe quickly enough for the total Fe concentration to rise to about 10^{-8} mol/L, ferrihydrite forms but lower rates of Fe release will not produce coatings (Huminicki & Rimstidt 2009). Thus, a stronger oxidant may be needed to accelerate release of Fe and coating formation.

2.4.2 Prior Study of the Prevention of Pyrite Oxidation Through Microencapsulation

Coating pyrite surfaces with a substance that cuts the contact between solution and the surface may prove to be a practical way to stop pyrite oxidation. A few types of pyrite coating have been investigated, including iron oxyhydroxide ((Huminicki & Rimstidt 2009), ferric phosphate (Evangelou (B) 1995), ferric hydroxide-silica (Zhang & Evangelou 1995; Kargbo et al. 2004), and phospholipids (Kargbo et al. 2004). There is compelling laboratory data to show that these coatings have reduced the pyrite oxidation rate effectively, but they usually require a large excess of reagent to ensure an effective coating.

2.4.2.1 Iron (oxy)hydroxide (Fe(OH)₃/FeOOH) coating Fe oxyhydroxide is developed naturally under high pH environments, which is supposed to be self-healing and become more and more effective as time goes by. Therefore, the demand for alkalinity addition would decline as coatings grow thicker and denser. In Huminicki and Rimstidt's investigation (2009), laboratory column experiments were conducted to simulate the treatment of AMD contaminated water. It was found in their investigation that the growth of solid coatings around mine residue surface is composed of two stages. (1) In initial stages, the production rate of Fe³⁺ is faster and the deposition of colloids is stemmed from the precipitates of Fe³⁺ at alkaline pH. Initially formed metastable Fe(OH)₃ and/or ferrihydrite would convert to goethite (Huminicki et al. 2009). This layer of deposits is thin and highly permeable, rendering it a physically weak barrier. This is justified by data showing that the rate of declination in the first 10 hours is very slow. (2) The second stage is speculated to be the propagation of the coating. In this stage, the Fe-oxyhydroxides precipitate in the pores of the first layer. Having the point of zero charge (PZC) at pH 1.4, normally pyrite is negatively charged. In contrast, the PZC of Fe-oxyhydroxide lies between 8 and 9, it usually slightly positive charged (Yee et al. 2006) . This offers theoretical support for the attraction and attachment of Fe-oxyhydroxide on the pyrite surface and the initial porous layer due to the electrostatic force. The Fe²⁺ released in the beginning of new pyrite oxidation would react with the oxidant diffusing in the permeable layer and being oxidized to Fe³⁺, which would in turn precipitate between the attached colloidal particles. The presence of Fe²⁺ is conducive to the transformation from poorly crystalline Fe-oxyhydroxide to goethite (Yee et al. 2006). In this way, the initial layer of Fe oxyhydroxide is refilled with the Fe oxyhydroxide formed in the second stage, becoming thicker and less porous. It is reported that the oxidant's diffusion coefficient is decreased by more than five orders of magnitude when such a coating is

in place. Once the dense layer of Fe oxyhydroxide is formed, the pyrite oxidation rate declines as the square root of time.

The solubility of iron (oxy)hydroxide is highly dependent on pH. In order to form a full solid and dense layer of Fe oxyhydroxide, a highly alkaline environment is required. Actually, such an alkaline environment is the key for triggering the formation of its first layer. Moreover, pH above 6 is required to neutralize the initial release of protons adjacent to the grain surface so that the deposit of Fe oxyhydroxide may be possible. In an experiment conducted by Zhang and Evangelou (1998), a formation of an amorphous ferric hydroxide coating on the grain surface was induced in the pH range of 4 to 6. This ferric hydroxide did interrupt the diffusion of H_2O_2 and other possible oxidants in the latter stage. But when the pH goes below 4, the pyrite oxidation was never inhibited due to solubility of amorphous ferric hydroxide under acidic pH. All these calls for maintenance of an alkaline environment in the very beginning, meaning that alkalinity addition is definitely required for successfully forming such a coating.

The study of Huminicki et al. (2009) on forming (oxy)hydroxide coatings is significant for it proves that inhibition by pyrite passivation may be possible. The key issue here is that, the encouraging results for the inhibition of pyrite oxidation were achieved in a laboratory environment, where the role of microorganisms was eliminated. Moreover, the data shown in their study only show the coating to be effective for the initial 13 hours, without determining whether it is still working afterwards. As a result, whether this coating yields the desired long-term prevention effect is unknown. It is critical to realize that ferric (oxy)hydroxide can precipitate either as a discrete phase or as a coating on pyrite surface, depending on Fe^{3+} activity (Moese et al., 1991, Nicholson et al., 1990). Further studies are still needed to explore its potential as an optimal coating.

2.4.2.2 Pyrite Passivation by Phosphate Iron phosphate, with a solubility product of 9.91×10^{-16} and low affinity to water, can be considered a good candidate coating agent. In Huang and Evangelou's (1994) investigation, coal waste was leached with phosphate at pH 5 to 7 in the presence of low concentration of H_2O_2 (0.147 mol/L) using NaAC as buffer. Aided by H_2O_2 , the conversion from Fe^{2+} to Fe^{3+} , the rate-limiting step, has been sped up. This promotes the ferric (oxy)hydroxide precipitation on the grain surface. With the introduction of phosphate with the concentration of 10^{-3} mol/L, approximately 40% of the pyrite remained unreacted after 1000 min of leaching at pH 4. In contrast, devoid of phosphate, the percentage of unreacted pyrite was 30%, which is accomplished with the deposition of ferric (oxy)hydroxide. This lends support to the formation of an enhanced coating and attachment due to the presence of phosphate. It may be seen from the demonstration above that, upon introducing H_2O_2 , Fe^{2+} in original pyrite has been oxidized to Fe^{3+} . For it is only the FePO_4 that is insoluble in liquid phase; the oxidation of Fe^{3+} is crucial for the latter coating formation. The Fe^{3+} would further react with phosphate and precipitate out on the grain surface. The investigations showed that the effectiveness of coating remained the same under various phosphate concentrations. When the phosphate concentration was increased from 10^{-4} M to 10^{-2} M, the percentage of pyrite remaining unreacted was the same (about 80%).

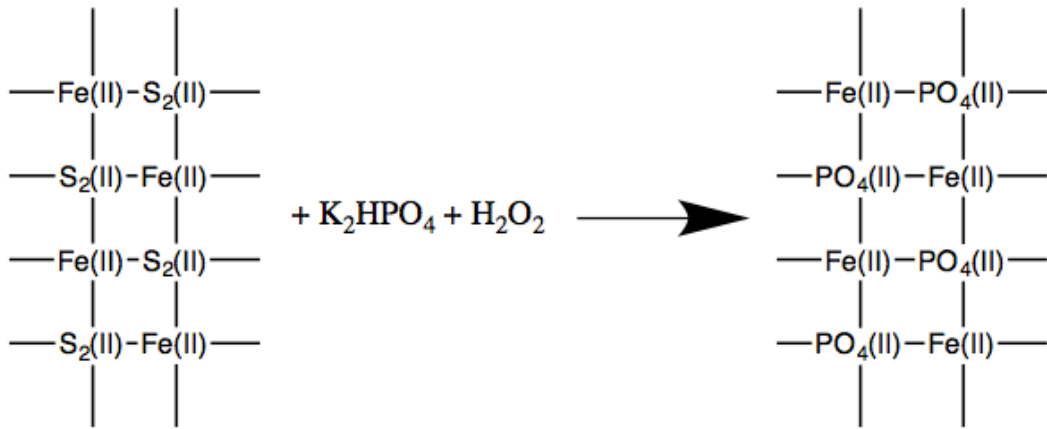


Figure 1 Schematic of Proposed Microencapsulation Technology (Evangelou, 1996)

The investigation of phosphate's possible role on pyrite passivation is important, for it showed that a coating other than ferric oxides may actually be developed. However, phosphate is not considered effective enough to achieve complete inhibition within an acceptable time. With formation of ferric phosphate, the effectiveness of coating, which is measured by the ratio of iron released with/without coating solution, is just promoted by 10%. Additionally, the introduction of phosphate may entail eutrophication once the leachates are discharged in the environment, for phosphate is the limiting nutrient for the growth of algae. Moreover, H₂O₂ is required to initialize a quick release of Fe³⁺ to promote its precipitation around the mine residue surface. The handling of H₂O₂ may be a source of difficulty in the field.

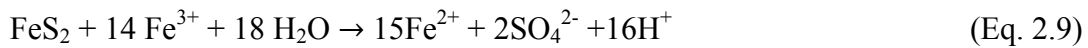
2.4.2.3 Pyrite Passivation by Phospholipid Experimental studies have been conducted with two-tail phospholipids, containing two hydrophobic tails per hydrophilic head group that form bilayers on the solid surface (Elsetinowa et al. 2003). In contrary to the application of single-tail lipids (e.g., stearic acid), which show little effect on suppressing pyrite oxidation, the amount of suppression of these lipids is as high as 80%. In light of the fact that water is a key element in the pyrite oxidation cycle, the hydrophobic pockets in bilayer structure interrupt the contact between pyrite surface and water. As a result, the reactivity of water in the pyrite oxidation is diminished. Further, the hydrophobic tail of the bilayer structure can serve to stabilize an adsorbed phosphate group and promote the binding between lipids and grain surface (Kargbo et al., 2004). Thus, a physical hydrophobic layer emerges and attaches firmly to the solid surface, providing a barrier to protect the pyrite surface from the oxidants in solution.

However, in a study designed to investigate the effect of silicates, the products of weathering of aluminosilicates minerals in mining environments, on their suppression on pyrite oxidation, Kargbo et al. (2004) determined that even at neutral pH, the presence of silicate suppresses phosphate lipids' ability to protect pyrite from being oxidized. When the pH is as low as 2, phosphate lipids performed poorly in coating the grain surface and a large amount of Fe^{2+} was induced as the oxidation of pyrite did not cease.

2.4.2.4 Pyrite Passivation with Silicate The relatively constant solubility of silica under various pH conditions (Lindsay 1979) and its relatively strong binding with Fe^{3+} due to the strong short-range interactions, have qualified it as a desirable candidate for the formation of a robust coating surrounding the pyrite surface (Evangelou et al. 1998).

It is postulated by Zhang and Evangelou (1998) that an iron oxide – silica coating can form a thick and dense layer on the pyrite surface in the pH range of 4-6. The solution for

developing the iron oxide – silica coating on pyrite surface was composed of H₂O₂ as an initial oxidant, sodium metasilicate as a coating material, NaOAC as a pH buffer, and NaCl as a background electrolyte. The concentrations of coating solution seem to have little influence on the inhibition of pyrite oxidation. H₂O₂ is also added to initialize a quick release of Fe³⁺ so that a stable precipitate Fe(OH)₃ can be expected. The reaction between pyrite and H₂O₂ under neutral pH carried out as following equations:



In the beginning stage of the experiment, the pyrite is oxidized by both H₂O₂ and Fe³⁺. The rate of pyrite oxidation is the sum of these two oxidation reactions.

When the pyrite is leached with the coating solution, the research results showed that 99% of iron release during the pyrite oxidation remained in the column as a precipitate. More importantly, rather than precipitating as a discrete phase in the solution, ferric oxides – silica is deposited on the grain surface, which is convinced by the results from a control group. The inhibition of pyrite oxidation is related to the formation of pyrite –iron oxide coating formed by the iron release from the pyrite (Evanleou & Seta 1998). This critical process heavily depends on pH. When pH is favorable (above 4), Fe³⁺ released initially precipitate around grain surface and subsequently interacts with silicate to form a denser coating—ferric oxide—silica. It is speculated by the researchers that silicate would react with OH group on grain surface to form a silicate precipitate, followed by further deposition of silicate ions on the silica precipitation. This results in the formation of negatively charged; open framework silica polymer that can either flocculate over or coat pyrite (Kargbo et al. 2004).

When pH is as low as 2, the results in their studies showed the pyrite inhibition is just 20% lower than that achieved in alkaline pH (Kargbo et al. 2005). According to Olson (Olson et al. 1973), a rather inert Fe^{3+} - monomeric silicic acid complex is formed between pH 1.5 to 3. This result is consistent with the results found in Weber and Stumm et al. (1965). Therefore, the inhibition effect of coating solution under acidic pH is attributed to the complexes formed. By using such silica coatings, the activity of a major oxidant on pyrite oxidation, Fe^{3+} , is dramatically reduced even at low pH. At the same time, the complex on the surface can also act as a barrier for the interaction between grain surface and oxidants. This complexation reaction is shown in **Equation 2.10**:



Using scanning electron microscopy (SEM), it was determined that pyrite grains were surrounded by a silica rim with a thickness of about 3mm. Moreover, the SEM micrographs showed that the coating took place on the entire framboidal cluster as well as on individual grains.

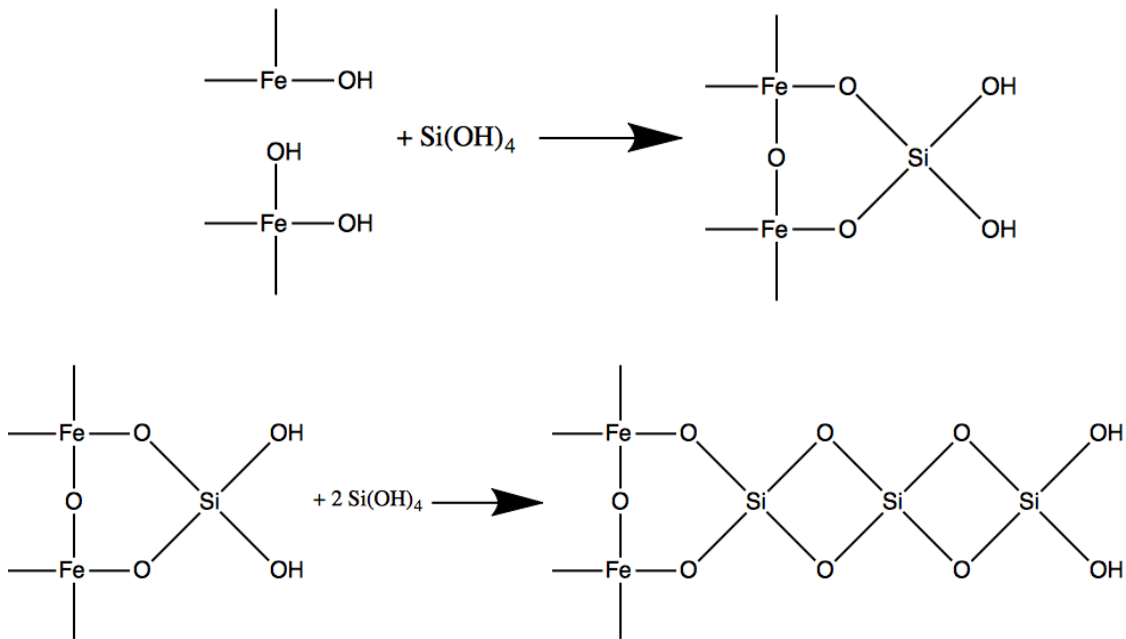


Figure 2 Schematic of Ferric Oxides - Silica Coating (Karbgo et al. 2005)

The durability and stability of coating formed with H_2O_2 and silicate is dependent on solubility of silica, which in turn is independent of pH once a certain K_{sp} is met. This K_{sp} is suggested to be variable, depending on the composition of silica surface and interaction between the silica surface and adsorbed components, such as Fe^{3+} (Iler 1979).

However, the idea concerning the coating formed under acidic pH is not fully evaluated and investigations done by Kargo et al. (2005) have questioned the existence of such a coating under low pH environments even though their data and results agree with silicate's effectiveness in suppression of pyrite oxidation at alkaline pH. The disagreement of the stability of coatings under low pH environments is based on the fact that the complex formed by Fe^{3+} and silica is known to dissolve at low pH (Kargbo et al. 2004). In their investigation, concentration of Fe released with addition of silicate is significantly higher than that of no silicate when pH is 2

(Kargbo et al. 2005). It is explained that at low pH, Fe^{3+} remains in solution either to form a soluble complex or to oxidize pyrite, exacerbating pyrite oxidation.

As a result, controversy remains on silicates' ability to form a stable layer of barrier with ferric oxide under low pH environments. This knowledge is essential for implementation on the industrial scale.

2.4.3 Summary

Every coating agent has strengths and limitations. To date, there is no ideal a coating solution advocated by researchers and mining companies for the inhibition of pyrite oxidation and AMD formation. Alkalinity addition is still a widely used field practice, which can be costly and ineffective. If alternatives such as microencapsulation can be implementable and established, the inactivation of pyrite could be long lasting and highly cost effective. No other technologies for treating AMD and pyrite can compete with these advantages. As a result, microencapsulation, one technology under development, is worthy of attention and effort for investigating. However, prior studies are limited to the lab scale: pure pyrite crystals were ground to a size less than 200 μm before being placed in a leaching column, with a bed thickness of about 3-4 mm, which is most likely not representative of field sites. What works in the lab environment and small scale is not guaranteed to work in the field application. This is governed by several factors not limited to but including the wide range of pyrite particle sizes, impurities in the mineral, and the geology of backfill. Moreover, it is difficult to predict the behavior of some chemicals in the field, such as H_2O_2 , a strong oxidant used for speeding up initial pyrite oxidation.

The aim of this thesis is to explore the potential of using wastewater (specifically hydraulic fracturing water) derived from shale gas extraction as an alkalinity provider in pyrite oxidation and its dynamic reaction with products from pyrite oxidation. It is known that a considerable amount of sulfate is expected to be in solution once the pyrite oxidation is initiated. On the other hand, there is plenty of Ba in fracturing water, which can react with sulfate and then precipitate on the mine residue surface. Meanwhile, due to the alkalinity provided by fracturing water, upon pyrite oxidation, ferric iron released will likely be immobilized as ferric oxides. The sedimentation of solid barium sulfate and ferric oxides upon the surface of mine residue can be considered an armor to prevent the further contact or interaction between mine residue and other oxidants, such as water and dissolved oxygen. The application of fracturing water can be significant for preventing the formation of AMD ultimately. At low pH, oxidation of pyrite by Fe^{3+} is dominant and very rapid and is catalyzed by acidophilic bacteria. As a result, if the low pH environment is addressed, the permanent treatment of AMD can be expected. This requires the rate of alkalinity addition to be faster than that of acidity production by pyrite oxidation, which can be accomplished using fracturing water. A second objective is to investigate the influence of the chelating agent GOPS as an additive to enhance the inhibition of pyrite oxidation in the presence of fracturing water. It is possible for GOPS to react with the ferric oxide produced in the earlier stage and form a stable coating with hydrophobic tails, which is ideal for prohibiting the contact between mine residue and all oxidizing agents. Overall, this work aims to determine the feasibility of establishing a stable and robust coating through the addition of GOPS in the presence of fracturing water to shut off electron transfer between pyrite surface and oxidants.

3.0 MATERIALS AND METHODS

3.1 INTRODUCTION

This chapter describes in detail the materials and methods used in the investigation of flowback water and GOPS as a potential treatment for acid mine drainage (as shown in table 2.1). Methods for the kinetic and equilibrium measurements are described, as are the sources of the various materials tested.

Table 1 Studies Conducted in This Thesis Program

Batch Studies	1. Selection of Ratio between Fracturing Water and Mine Residue
	2. Selection of Equilibration Time
	3. Effect of H ₂ O ₂ on Suppression of Pyrite Oxidation
	4. Effect of GOPS on Suppression of Pyrite Oxidation
Column Studies	1. Control Column Studies
	2. Test Column Studies

3.2 MATERIAL AND SAMPLE PREPARATION

3.2.1 Solutions and Other Chemicals

All chemical used were ACS grade: Barium chloride dihydrate (99.0% min, Mallinckrodt Chemicals), acetic acid (99.0%, Fisher Scientific), sulfuric acid (95-98%, Acros) and GOPS (Z-640, Dow Corning).

Standards for calibration of atomic absorption spectroscopy (AAS) and ion chromatography (IC) were prepared from standard solutions purchased from Fisher Scientific. The range of iron (Fe) standards used was 0.1, 0.25, 0.5, 1, 5, 10, 15 and 20 mg/L, the range of barium (Ba) standards used was 1, 3, 5, 10, 15, 18, and 20 mg/L, and the range of sulfate (SO_4^{2-}) standards used was 10 – 60 mg/L.

3.2.2 Source of Mine Waste and Flowback Water

The mine residue used in this study was obtained from Mather Mine, Mather, PA and provided by Alcoa Inc. The X-ray diffraction (XRD) report on the mine residue provided by Alcoa Inc. provides a rough material description and is summarized in **Table 2**. Mine residue was stored under ambient conditions in a 55 gallon drum prior to experimental runs.

The flowback water used in this study was obtained from a hydraulically fractured well at the Slack 2H drilling site operated by Consol Energy. For the batch tests day flowback water from day 5 of drilling was used, while for the column tests water from day 1 of drilling was used (day 1 flowback water comes from the first day of flowback after pressure is released on the well,

while day 5 flowback water comes from day 3.) Day 1 flowback water contains less total dissolved solids (TDS) than day 5 does.

Table 2 Composition of Mine Residue from The Mather Mine

Major	Quartz, SiO ₂ ; Muscovite, KAl ₃ Si ₃ O ₁₀ (OH) ₂
Minor	Kaolinite, Al ₂ (Si ₂ O ₅)(OH) ₄
Very Small	Jarosite, K(Fe ₃ (SO ₄) ₂ (OH) ₆) or Alunite, KAl ₃ S ₃ O ₁₀ (OH) ₂
Trace	Titanium Oxide, TiO ₂ ; Gypsum, CaSO ₄ ; Iron Sulfide, FeS ₂
Trace Possible	Goethite, FeO(OH), Calcium Carbonte, CaCO ₃

3.2.3 Preparation of Mine Waste and Flowback Water

The particle size distribution of mine waste samples was determined using sieve screens according to the protocol ASTM D 422 - Standard Test Method for Particle-Size Analysis of Soils, summarized below. After making sure that all the sieves are clean, the weight of each sieve as well as the bottom pan was recorded. A subsample of mine residue was prepared and weighed. The sieves were assembled in the ascending order (#4 sieve at top and #270 sieve at bottom). The mine residue sample was transferred to the top sieve, and the apparatus mechanically vibrated using a shaker for 30 minutes, which was sufficient for separation to take place. For the batch tests, particles below 19mm only were used to mimic the worst-case scenario, while for the complete distribution of particles was used for the column tests. Notably, Orndorff et al. (2010) observed that for the leaching column experiment, their study revealed no significant difference between coarse and fine refuse materials for any parameter of long term leaching concern.

Flowback water samples were used in their natural state ('as received') with no chemical modification.

3.3 EXPERIMENTAL PROCEDURES

3.3.1 Batch Studies

The core protocol for batch studies is described in this section. Components of this core protocol were varied for individual tests as described below. 500 mg of mine waste was suspended in 55 mL of flowback water in a 300 ml glass beaker. The mixture was agitated for 30 min using a magnetic stirring machine, and afterwards allowed to settle for 30 min. The mixture was then filtered through filter paper with pores of 0.65 μm . The filtrates were stored at room temperature prior to analysis. pH was measured using a pH meter, Ba and Fe concentration were measured AAS, and SO_4^{2-} concentration was measured using IC.

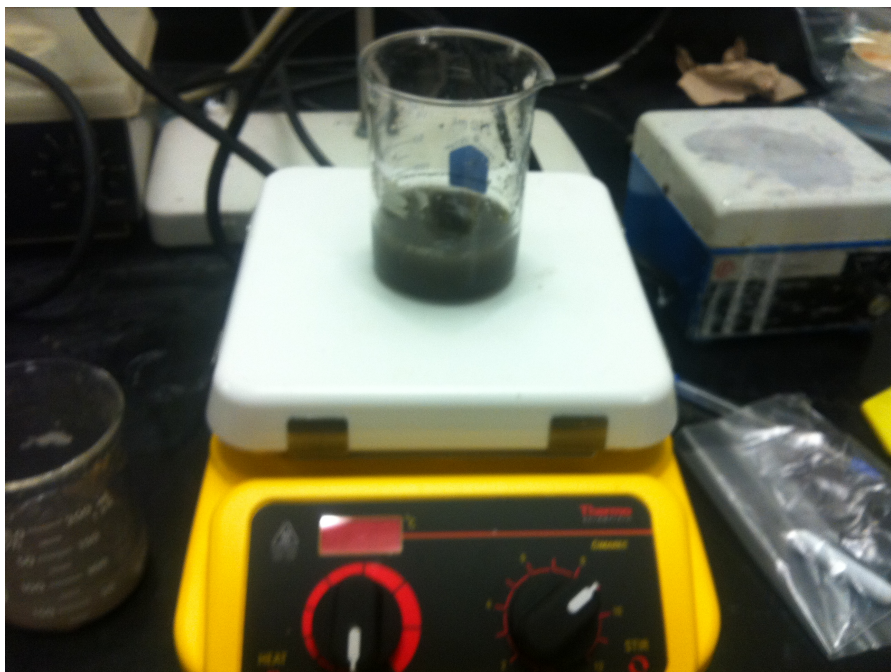


Figure 3 Schematic of Bathc Apparatus

3.3.2 Volume of Flowback Water

The appropriate ratio of flowback water to mine residue that induce the lowest levels of concerned contaminants, was determined by adding different volumes of flowback water to a fixed 500 mg volume of mine residue. Volumes of 8, 16, 25, 30, 35, 40, 45, 50, 55, and 60 mL were tested. pH was measured prior to addition for samples of volume 40, 45, 50, 55, and 60 mL, and afterwards for the 40 and 60 mL samples. All samples were analyzed using AAS and IC.

3.3.3 Duration of Mixture Agitation

The incubation time of the flowback water/mine residue mixture was determined by varying the duration of agitation by magnetic stirrer. Agitation times of 15, 30, 45, and 60 minutes were

tested. All samples were allowed to sit for 30 min prior to filtration. The filtrates were analyzed via pH measurement and AAS.

3.3.4 Effect of Hydrogen Peroxide

The effects of treating mine residue with a combination of flowback water and hydrogen peroxide (H_2O_2) were tested using solutions with various concentrations of H_2O_2 . 55 mL of H_2O_2 solution of varying concentration was added to 55 mL of flowback water, allowed to mix for 1 min, and then added to 500 mg mine residue and analyzed using the standard protocol. H_2O_2 solutions of concentration 0.142, 0.284, 0.426, 0.568, 0.710, 0.852, 0.994, 1.142 M were tested and prepared from 30% wt/vol stock from Fisher Scientific. The filtrates were analyzed via pH measurement, and AAS.

3.3.5 Effect of 3-glycidoxypropyltrimethoxysilane (GOPS, $\text{C}_9\text{H}_{20}\text{O}_5\text{Si}$)

The effects of treating mine residue with a combination of flowback water and 3-glycidoxypropyltrimethoxysilane (GOPS) were tested using solutions with various concentrations of GOPS. GOPS concentrations of 10^{-5} , 10^{-4} , 10^{-3} , 10^{-2} , and 10^{-1} ppm were tested and prepared from pure liquid stock obtained from Dow Corning® (Z-6040 Silane). An acidic solution of pH 4.0 was prepared with pure acetic acid obtained from Fisher Scientific. Acetic acid was added into a 1000 ml beaker of deionized water with stirring until the pH reached 4.0 ± 0.01 . Different volumes of GOPS were added into this acidic solvent to prepare stocks of different concentrations. The mixtures of GOPS and acidic solvent were stirred for 15 min.

150ml beakers were filled with the standard amounts of 500 mg mine waste and 55 ml flowback water, followed by mixing for 30 min. GOPS solutions of various concentrations were then added to the mixture and stirred for an additional 45 min. This was followed by 30 min of sitting prior to filtration. Samples were analyzed by pH meter, AAS, and IC.

3.3.6 Effect of Hydrogen Peroxide and GOPS

The effects of treating mine residue with a combination of flowback water, H₂O₂, and GOPS were tested using solutions with various concentrations of GOPS. To a mixture of 55 mL of flowback water and 55 mL of 0.142 M H₂O₂ in a 200 mL beaker were added 500 mg of mine residue. The mixture was stirred using a magnetic stirrer for 45 minutes, while GOPS solutions were prepared as described above. GOPS concentrations of 10⁻⁵, 10⁻⁴, 10⁻³, 10⁻², and 10⁻¹ ppm were tested. GOPS was added to the samples, followed by an addition 45 min of stirring. The samples were allowed to sit for 30 min prior to filtration, followed by analysis by pH meter, and AAS.

3.3.7 Column Studies

Large-scale fluidized bed column experiments were carried out using an apparatus shown in **Figure 3**. A laboratory-scale Plexiglas columns of inner diameter 6 in and height 28 in was connected to a pump and storage tank using plastic drainage pipes. The ends of the column and storage tank were sealed using plastic wrap (Rite Aid) to prevent loss of water from the column due to the high flow rate of pumping. The liquid was fed into the bottom of the column in an

upward flow motion using a pump (Grainger SHURFLO Pump 4UN56). Upward flow was chosen to maximize the contact between grain surface and fluid and too prevent the formation of channels while the column is running. 150 g of mine residue was packed into the column. Mine residue was carefully prepared using the measured particle-size distribution of the complete mine residue sample. Based on the 55 mL of flowback water used for 500 mg of mine residue in the batch studies, 16.5 L of flowback water was used in column studies. The system was flowed continuously, and samples of volume 30 ml were obtained once per day. A control column was prepared identically and treated using deionized water. The experimental column was run for 30 days, while the control column was run for 15 days. For each sample, pH was measured immediately, the samples were filtered through 0.65- μm pore Teflon filters using a vacuum filter, followed by analysis by AAS and colorimetry.

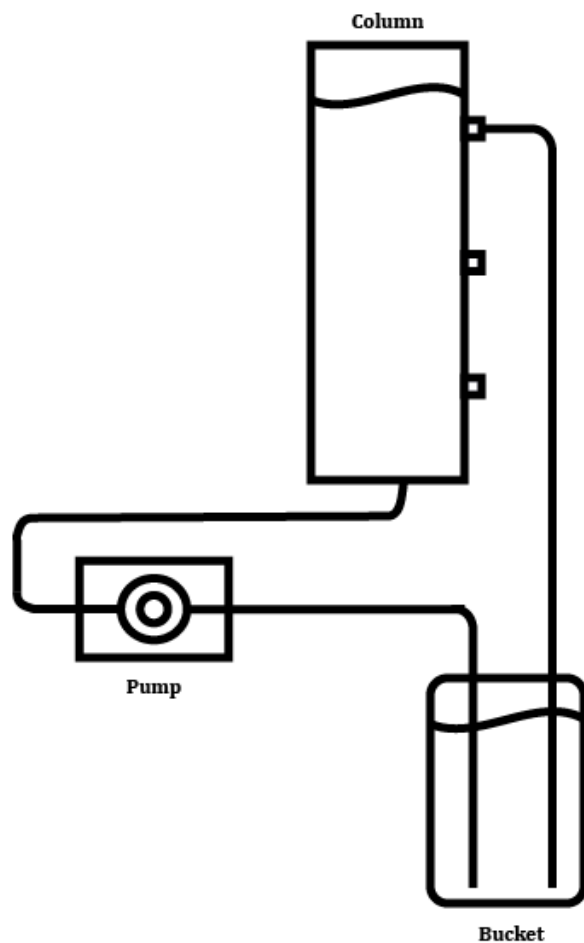


Figure 4 Schematic of Column Apparatus

3.4 SAMPLE ANALYSIS

Following filtration, samples were stored in sealed sample tubes/bottles. For batch studies, pH was measured using a pH meter (Fisher Scientific, S90526). For both batch and column studies Ba and Fe levels were measured using an AAS, (Model 751, Instrumentation Laboratory, USA) according to ASTM standard methods (300X for metals 4500 for anions). The AAS uses an air–

acetylene/air-acetylene-nitric gas flame and single element hollow cathode lamps. The concentrations of some samples exceeded the range of the AAS instrument; these samples were diluted with deionized water before detection. The AAS instrument was calibrated using standard solutions of the respective metals in the range of 0.1 – 20 mg/l. AAS measurements were the average of three duplicate measurements, which were within 5%. For batch studies, the concentration of SO_4^{2-} was measured using ion chromatography (IC). The IC makes use of a resin to separate different ions and allows measurement of their concentrations via peak area. Samples were diluted appropriately to make sure that their concentrations were in the detection limit. The IC instrument was calibrated using standard solutions in the range of 10 – 100 mg/L. The IC measurements were the average of three duplicate measurements. For column studies, the concentration of SO_4^{2-} was measured using a DR/890 Portable Colorimeter (Hach, 4847000). All the samples were diluted accordingly to make their concentrations within 80mg/L, which was the detection limit of the colorimeter. These measurements were only conducted once. X-ray diffraction (XRD) measurements were conducted externally by the lab of Alcoa Inc.

4.0 RESULT AND DISCUSSION

4.1 INTRODUCTION AND OBJECTIVE

In this chapter are described the batch-scale tests conducted to select design parameters for the main large-scale column tests are described. Previous studies testing other coating agents such as phosphate (Huang & Evangelou, 1994) and silicate (Kargbo et al., 2005, Zhang & Evangelou, 1998) have been conducted using pure pyrite particles less than 250 μm in size and at small scale, using columns 5.7 cm in diameter and 50 cm in height. The work done herein was conducted using real mine residue and a larger column 15.2 cm in diameter and 71 cm in height in order to more closely mimic real-world usage.

4.2 BATCH STUDIES

4.2.1 Sieve Analysis

The raw mine residue used in these studies consisted of a mixture of particles of different sizes. The particle size distribution was measured using sieve analysis, in which a series of filters of varying pore sizes are used to filter the residue. The results of this analysis are shown in **Table 3**

and **Figure 4**. For the large-scale column studies, mine residue was to be prepared using the method of probability proportional to size (PPS). The particle size distribution was measured for a total of 11.37 kg of mine residue, split into 10 samples and averaged. Approximately 78.7% of particles in the mine residue were larger than 19 mm in size, while approximately 4% of particles were smaller than 75 μm . For the column tests this distribution was then recreated manually from separate sieve fractions.

Table 3 Particle Size Distribution of Mine Residue from Mather Mine

Sieve Opening (μm)	Mass Retained (g)	Mass Retained (%)	Cumulative Mass Retained (%)	Mass Finer (%)
19000	2420.83	21.30	21.30	78.70
9500	2034.06	17.90	39.19	60.81
4750	2183.19	19.21	58.40	41.60
2000	2125.95	18.70	77.10	22.90
841	1228.43	10.81	87.91	12.09
420	452.16	3.98	91.89	8.11
250	223.79	1.97	93.86	6.14
150	155.94	1.37	95.23	4.77
75	276.51	2.43	97.66	2.34
53	52.19	0.46	98.12	1.88
<53	206.01	1.81	99.94	0.06

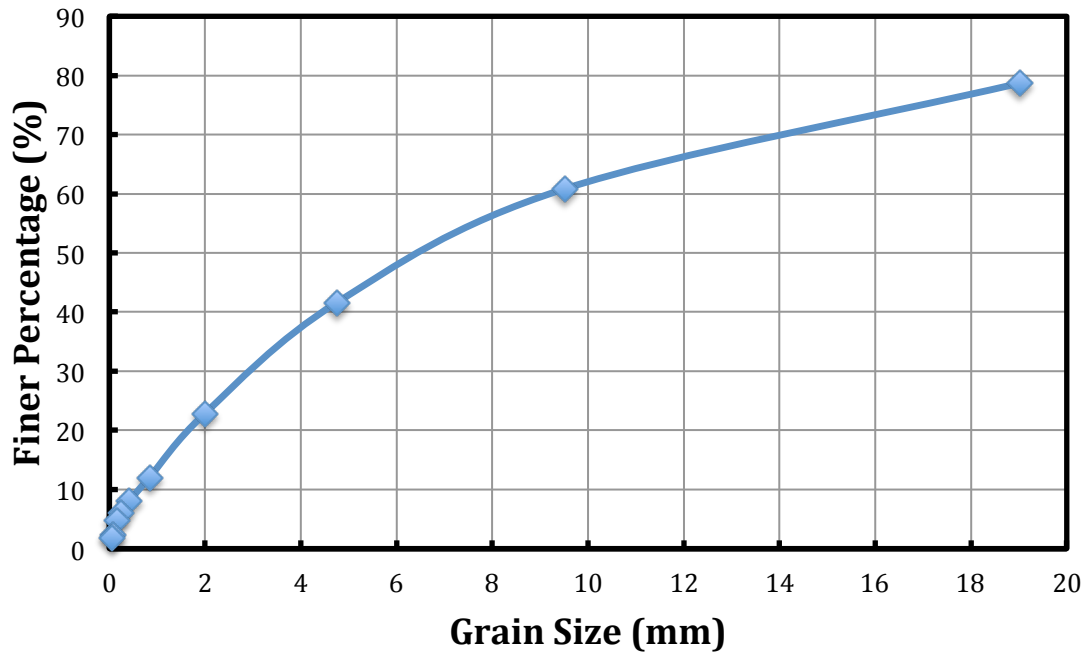


Figure 5 Particle Size Distribution of Mine Residue from Mather Mine

For the batch studies, in order to mimic a “worst-case scenario” only particles of less than 53 μm were used. These have the greatest specific area and thus highest expected reaction rate. Activation energies for pyrite oxidation by both ferric iron and molecular oxygen at room temperature are reported to be between 50 to 92 kJ/mol (Evangelou, 1995 (B)). These high activation energies indicate that the pyrite oxidation is a surface-controlled reaction, which has been well investigated (Kargbo et al. 2005; Zhang & Evangelou, 1998; Evangelou, 1995). As a result, the specific area is of great importance for the reaction rate. The higher volume to surface area ratio, the more availability of the surface under attack by ferric iron, oxygen and acidophilic bacteria.

4.2.2 Selection of Ratio Between Fracturing Water and Mine Residue

The generation of acid mine drainage may be reduced by the addition of an alkaline solution, such as the flowback water used in this work. The alkalinity present in the added solution neutralizes the acidity produced by pyrite oxidation. In addition, flowback water induces the formation of a coating on the mine rock surface that prevents the oxidation of additional pyrite. Iron (oxy)hydroxides grow around the mine rock surface and form a thick and stable coating.

In low pH conditions, pyrite is mainly oxidized by ferric irons (Fe^{3+}), which are generated by microbes from ferrous iron (Fe^{2+}) in solution. However, in higher pH conditions (>4), the solubility of ferric iron is low and the only oxidant available for pyrite is dissolved oxygen. This oxygen may be blocked from contacting pyrite through the formation of surface coating.

Concern may be raised about whether the precipitates will become suspended in the liquid phase instead of depositing on the coating of the surface of the mine rock. This is controlled by the high total dissolved solids (TDS) present in the flowback water, which give it a high ionic strength. Caldeira et al. (2003) observed that when pyrite is treated with high concentration of alkaline solution (Na_2CO_3), a discontinuous and coarse granular oxide coating formed initially on the grain surface, followed by further deposition by oxides on the existing nuclei. In contrast, when a low concentration of alkaline solution was applied, the grain surface was covered by only a thin layer of precipitates, which broke down after some time with the majority of precipitates suspended in the bulk solution. Thanks to the high ionic strength of flowback water, the thickness of the electrical double layer of particles suspended in solution is reduced, thereby favoring the coagulation at the grain surface, which acts as a seed for further precipitation and the growth of the oxide layer. Therefore, instead of precipitating and

suspending in the liquid phase, the precipitates formed (iron (oxy)hydroxides and barium sulfate) all contribute to the microencapsulation for prevention of further pyrite oxidation. Additionally, the variety of chemicals present in the flowback water allows the possibility of heterogeneous nucleation.

Unfortunately, the presence of barium in the flowback water sets an upper limit on the volume that may be used to neutralize AMD. At low amounts of flowback water, barium reacts with sulfate in solution released by the oxidation of pyrite. However, as the iron coating takes effect, the release of sulfate is slowed, and adding additional flowback water yields only a higher TDS, which should be avoided. Thus, it is necessary to determine an appropriate ratio between flowback water and mine residue, which favors the lowest level of all pollutants in the liquid phase.

In order to determine the optimal ratio the amount of iron, barium, and sulfate were measured in solutions prepared using different volumes of flowback water and constant mass of mine residue. The results are shown in **Figure 6**. In order to account for the varying volume of flowback water, the results are shown in terms of mass rather than concentration. The mass is the result of the concentration times volume. Additionally, the pH of several samples was measured. These samples are tabulated in **Table 4**.

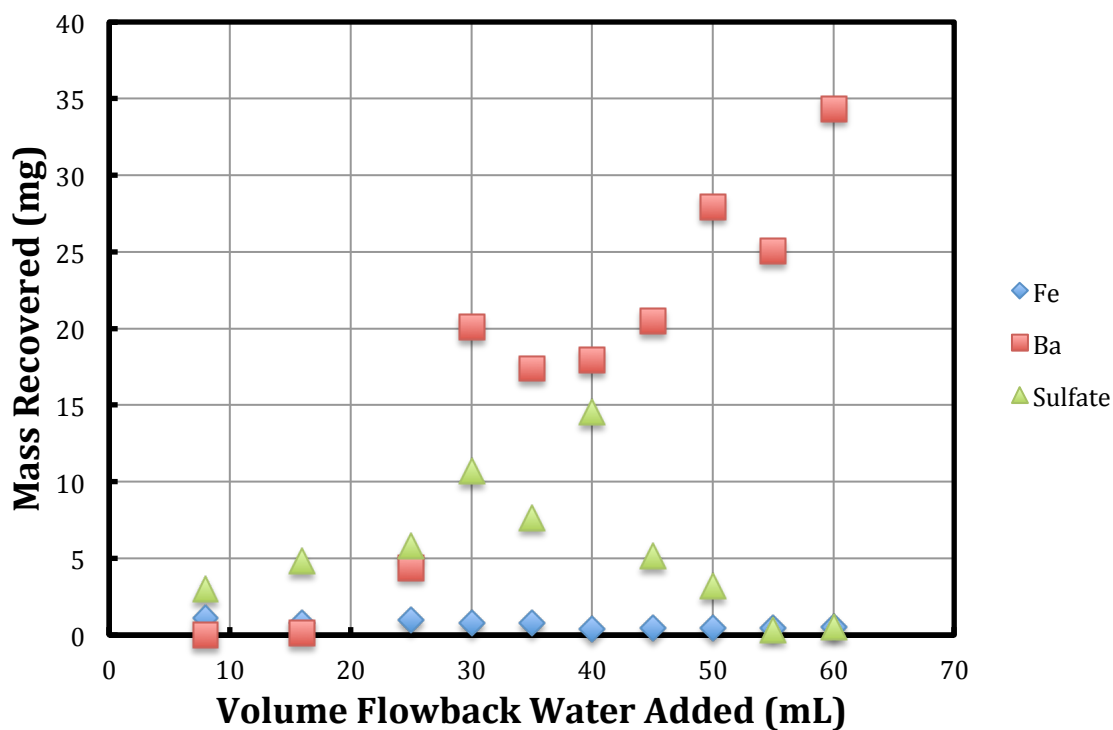


Figure 6 Mass of Fe, Ba, and SO₄²⁻ Recovered vs. Volume Flowback Water Added

Table 4 pH of Flowback Water and Deionized Water vs. Volume of Fluid Added

Volume of Fluid Added (mL)	Flowback Water pH	Deionized Water pH
40	6.196	4.227
45	6.122	-
50	6.402	-
55	6.617	-
60	6.737	3.564

The ratio of sulfate to iron present is greater than would be expected based on the composition of pyrite. This is explained by iron's formation of insoluble products such as ferric hydroxide ($\text{Fe}(\text{OH})_3$) and ferric oxyhydroxide (FeOOH), which are the major compositions of coating layers on the mine residue.

The comparison of pH between flowback water and deionized water also supports the reduction of pyrite oxidation through the formation of iron (oxy)hydroxide coatings. With deionized water, the pH of filtered sample after mixing for 60 min was as low as 3.5, while that reacted with the same volume of flowback water was about 7, which is acceptable by DEP regulation. The pH is a crucial parameter, for pH plays a vital role in the growth and activities of iron oxidizing bacteria, which facilitates the turnover rate of ferrous iron to ferric iron.

As can be seen in **Figure 6**, the mass of iron recovered shows an obvious trend of decreasing with increasing volume of flowback water. This can be explained in two ways. First, pH has reached about 7, the Fe released by pyrite has been excluded from the liquid phase by forming iron (oxy)hydroxide precipitates. Second, the pyrite has been coated by the iron (oxy)hydroxides, which eliminates the further release of Fe from the mine residue surface. When 55 mL of flowback water was added, the concentration of Fe was detected to be less than 1 mg/L.

When 7 mL and 14 mL of flowback water were added, the mass of Ba present did not increase, while the amount of sulfate present increased slowly. However, once a threshold amount of flowback water has been added (above 25 mL), the mass of Ba recovered begins to increase linearly with increasing volume of flowback water added, but with a decreasing amount of sulfate. This is explained by a combination of two effects. As flowback water is added, the increase in pH increases the rate of pyrite oxidation, increasing the sulfate concentration.

However, sulfate in solution precipitates with barium added with the flowback water, causing the observed behavior. The K_{sp} of barium sulfate is just 1.08×10^{-10} . As a result, as flowback water is added, the solution become supersaturated (more than 25 mL of flowback water was added), causing barium sulfate to deposit on the surface and helping to form the coating. In the supersaturated or labile zone, where the concentration of the solution is above the solubility curve, spontaneous nucleation followed by rapid crystal growth occurs.

Overall, these results suggest an optimal volume of flowback water of 55 mL in 500 mg of mine waste, with the best balance between low sulfate concentration and high barium concentration. It should be noted that in complicated cases such as the one here, coprecipitation may be expected, where other precipitates, such as those of aluminum and magnesium, may be incorporated into barium sulfate or iron (hydro)oxides' lattice and be removed from the liquid phase.

4.2.3 Selection of Equilibration Time

In order to select an appropriate equilibration time for further batch-scale trials, tests were run using various reaction times. Test samples were stirred for various amounts of time after addition of flowback water, while control samples were treated identically after addition of deionized (DI) water. The results show 30 minutes of equilibration with stirring to be sufficient, and validate the pH-neutralizing effect of adding flowback water.

Table 5 pH in Flowback Water and Deionized Water vs. Reaction Times

Reaction Time (min)	Flowback Water pH	Deionized Water pH
0	7.718	7.000
15	6.772	3.745
30	6.896	3.535
45	6.983	3.655
60	6.748	3.605

Table 6 [Fe] in Flowback Water and Deionized Water vs. Reaction Time

Reaction Time (min)	Final Concentration in Deionized Water (ppm)	Final Concentration in Flowback Water (ppm)	Reduction (%)
15	11.4	1.52	86.63
30	13.35	1.18	91.14
45	14.25	0.63	95.58
60	10.33	1.91	81.55

Table 7 [Ba] in Flowback Water and Deionized Water after Various Reaction Time

Reaction Time (min)	Initial Concentration in Flowback Water (ppm)	Final Concentration in Flowback Water (ppm)	Reduction (%)
15	997.15	175.71	82.38
30	997.15	391.17	60.77
45	997.15	190.08	80.94
60	997.15	477.35	52.13

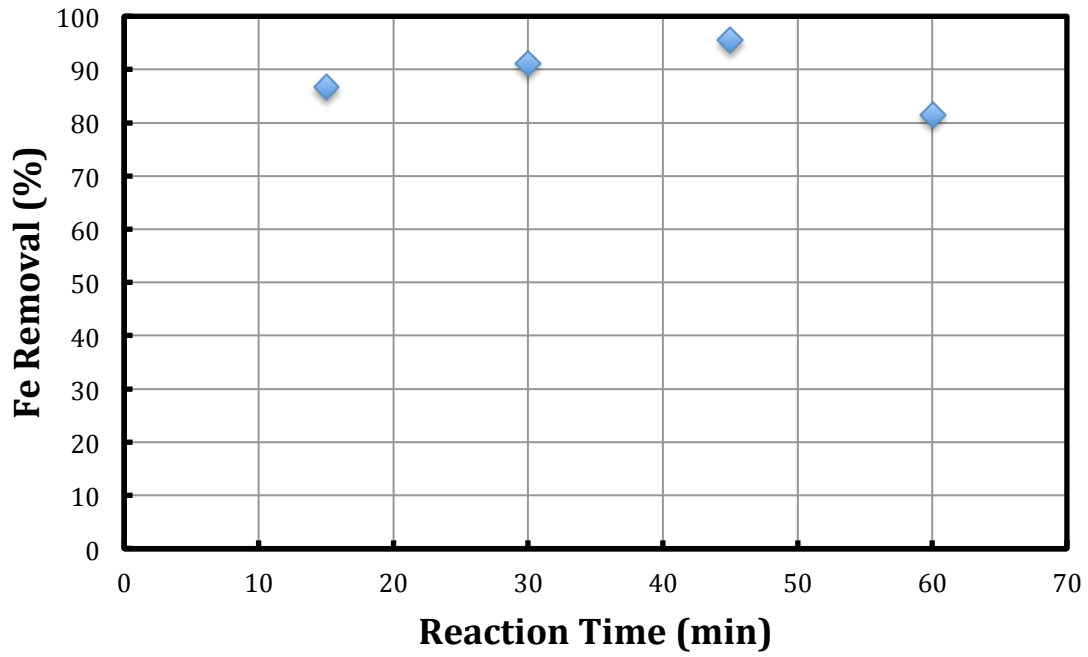


Figure 7 Fe Removal vs. Time

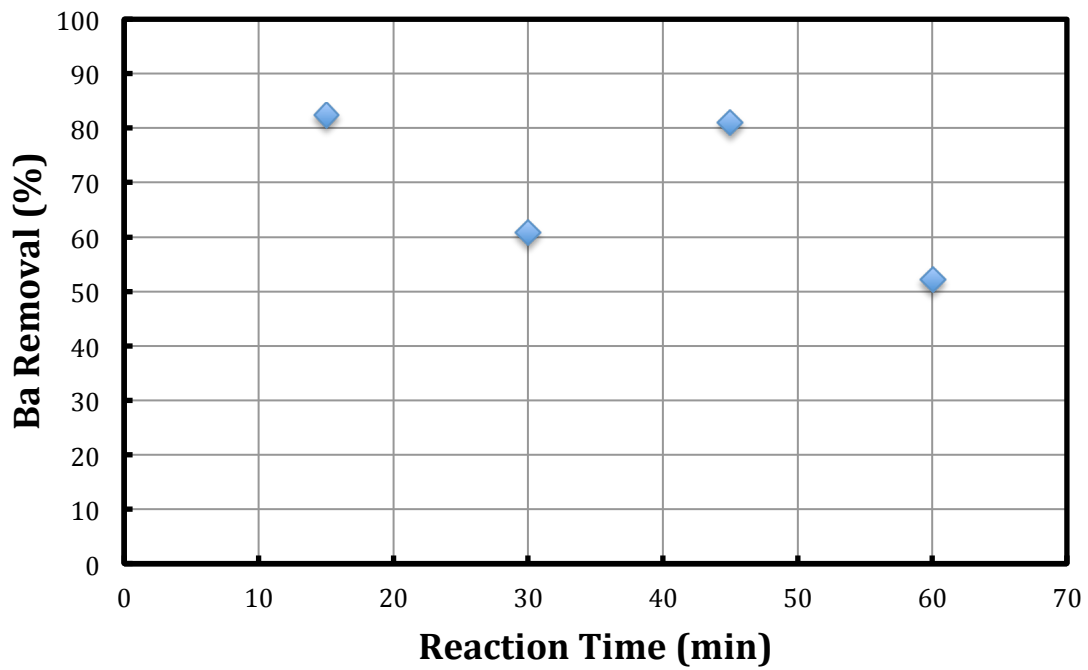


Figure 8 Ba Removal vs. Time

As shown in **Table 6**, the amounts of Fe released after treatment with DI water and flowback water were effectively the same over the equilibration times tested, about 13 mg/L and 1 mg/L respectively. Also, as shown in **Figure 7**, the removal percentage after different reaction times stays constant at about 90%. These results indicate that homogenous mixing was achieved within the shortest time tested. Although variation of [Ba] was observed among different reaction times, it can still be seen that the removal percentages were still relatively stable. The variation of Ba removal percentage may be attributed to instrumental noise.

Based on the results from the previous section, it is expected that for these tests conducted with 55 mL of flowback water, little or no sulfate would be observed. For all four tests, no sulfate was detected by Ion Chromatography (IC). Further confirmation of absence of sulfate was done by addition of 25mg/L and 50 mg/L of barium chloride. This yielded no precipitation after strongly shaking the mixture for 2 to 3 min, which would have been expected had sulfate been present. In conclusion, the experimental samples were equilibrated within 30 minutes, and further experiments were conducted using equilibration times of 30 to 60 min, followed by settling for another 1 hr.

4.2.4 Effect of H₂O₂ in Suppression for Pyrite Oxidation

In order to evaluate the potential of treatment with hydrogen peroxide (H₂O₂) in addition to flowback water to form an iron oxide coating on mine residue, tests were conducted with various H₂O₂ concentrations. The strong oxidizer H₂O₂ was chosen and added into the system of flowback water and mine residue after their ratio has been selected as described above. The

addition of H₂O₂ was designed to accelerate the release of Fe³⁺ and maximize the formation of its precipitate iron (oxy)hydroxides.

H₂O₂ attacks the mine residue surface and during coating formation oxidizes disulfide (S₂²⁻) to sulfate SO₄²⁻. The additional release of SO₄²⁻, as shown in **Figure 9**, may additionally help with the removal of Ba added as part of the flowback water. **Figure 9** demonstrates the effect of H₂O₂ on the pyrite, which includes favoring formation of Fe²⁺ over Fe³⁺. Compared with Fe²⁺, Fe³⁺ is more favorable as its precipitates Fe(OH)₃ and FeOOH are more stable than ferrous iron's precipitate Fe(OH)₂. This stability should be transferred to the coating layer, decreasing the chances that it will fracture or dissolve back into the bulk solution.

According to the theoretical chemical equilibrium equation, and assuming that the 500mg of mine residue tested was all pyrite (FeS₂), stoichiometrically 0.142 mg/L of hydrogen peroxide are needed for 55 mL of flowback water. Two, five times, and ten times of this stoichiometric amount were added to find the optimal concentration. The measured iron and barium concentrations of these tests are shown in **Figures 9** and **10**, while the pH are shown in **Table 8**.

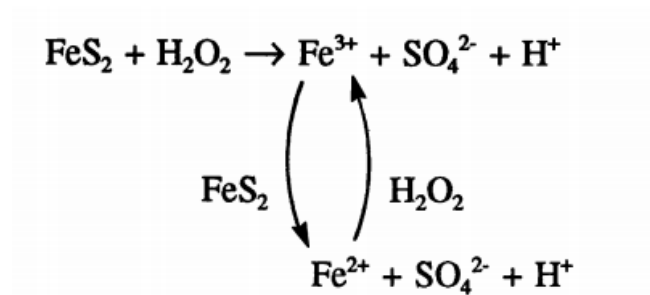


Figure 9 The interaction between H₂O₂ with Fe³⁺ and Fe²⁺ (Evangelou, 1995 (B))

Table 8 Effect of Hydrogen Peroxide Treatment on pH

H₂O₂ Conc. (ppm)	pH
0.142	7.360
0.284	7.222
0.716	7.012
1.418	6.497

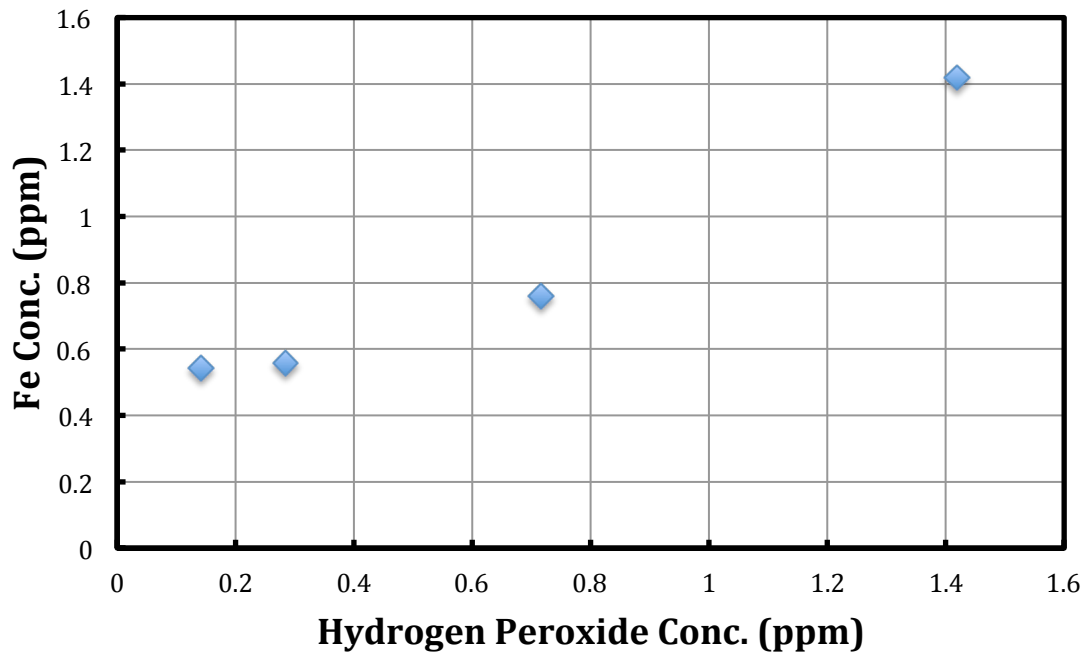


Figure 10 Effect of H₂O₂ Treatment on [Fe]

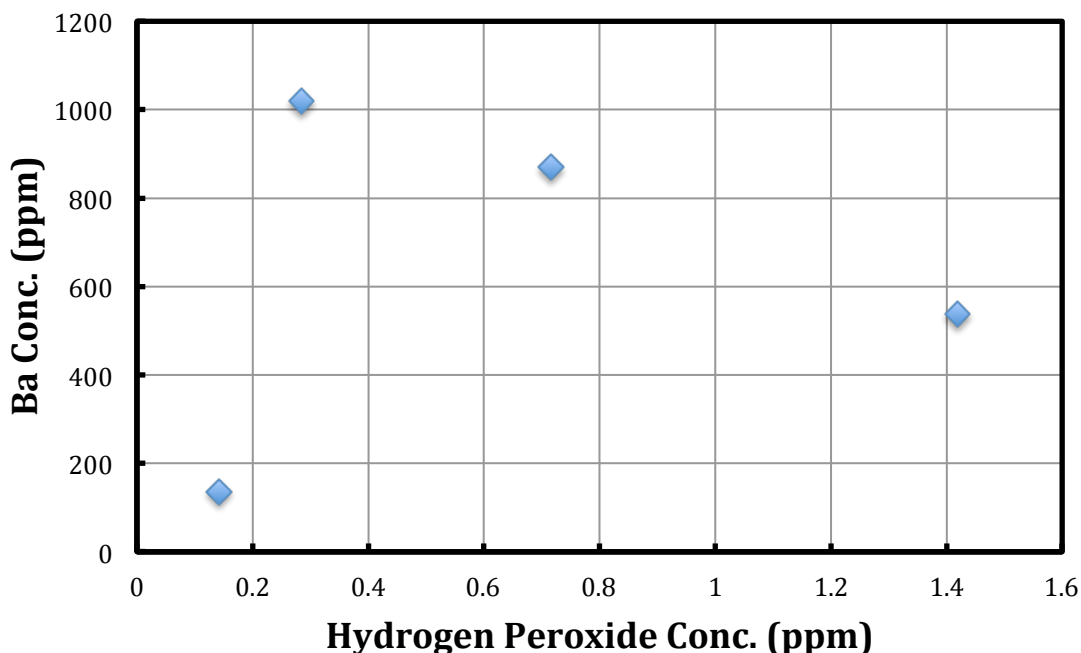
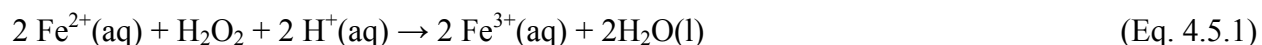


Figure 11 Effect of H₂O₂ Treatment on [Ba]

As can be seen in **Table 8**, the pH of all samples was near 7, and pH decreased with increasing H₂O₂ concentration. Part of the reason for the decreasing pH may lie in the following reaction:



This reaction is crucial for maintaining the alkaline pH environment and converting reduced Fe²⁺ to Fe³⁺, which will favor the formation of insoluble iron oxides developing and growing on the surface directly and eliminate the possible role of acidophilic bacteria in the system.

Based on the curves shown in **Figure 10** and **11**, as the concentration of H₂O₂ added was raised to two, five times, and ten times stoichiometric equivalence, the formation of iron oxides on the surface was actually less efficient, as the concentration of iron in solution increased

linearly. Barium concentration in solution increased initially, but at the highest concentration of H_2O_2 decreased. It is hypothesized that, when the concentration of H_2O_2 is within the reasonable and ideal range ($< 0.142 \text{ mg/L}$), the rate of ferric iron production is less than or equal to the rate of its consumption (binding hydroxyl OH^-) to precipitate out of the bulk. Beyond of this range the rate of pyrite oxidation exceeds of that of the formation of iron oxide coating. When this happens, an increase of iron and sulfate, the major products of pyrite oxidation, may be expected. As a result, barium concentration decreased with increasing sulfate concentration.

When $0.142 \text{ mg/L H}_2\text{O}_2$ was added to the liquid phase, it encouraged the initial oxidation of pyrite, releasing sulfate and ferric iron. The sulfate precipitated out with abundant barium from flowback water, while ferric iron precipitated out with hydroxyl. When the concentration of hydrogen peroxide reached 0.284 mg/L , more iron oxides and barium sulfate have deposited and covered the grain surface, blocking the interaction between mine residue and oxidant. Consequently, pyrite oxidation was suppressed and less sulfate was released, which agrees with the peak of barium concentration occurring at this point. At the same time, the concentration of iron remained the same as that when concentration of hydrogen peroxide was 0.142 mg/L in the solution. With the concentrations of H_2O_2 were above 0.142 mg/L , the balance between pyrite oxidation and coating formation has been upset. The increase of H_2O_2 concentration in the solution has encouraged the pyrite oxidation, increasing the release of iron into the bulk, which is supported by **Figure 10**. Meanwhile, the fact that too much H_2O_2 is harmful for the formation of coating can also be supported by the decrease of barium in solution, which is due to the precipitation with continuous release of sulfate from pyrite oxidation.

Through the testing of sulfate in these samples with IC, no sulfate was found in these four samples. The absence of sulfate in these samples was further confirmed by adding high

concentration of barium chloride. No precipitation was seen after shaking the mixture for about 5 min, as would be expected if sulfate were present. As mentioned in section 2, the sulfate produced may be consumed immediately in the flowback water containing high concentration of barium due to the low K_{sp} (1.08×10^{-10}).

When the concentration of hydrogen peroxide reached 0.284 mg/L, a stable iron oxides coating formed. But in this case, iron is not the only concern; the concentration of barium should also be lowered to an acceptable level. As a result, hydrogen peroxide, which works well in other studies (Evangelou, 1995 (B)) was not adopted for the column studies.

4.2.5 Effect of GOPS on Suppression of Pyrite Oxidation

It is hypothesized that the addition of the chelating agent 3-glycidoxypropyltrimethoxysilane (GOPS) in addition to flowback water will improve coating formation on mine residue. The structure of GOPS is shown in **Figure 12**. Previous research has explored the use of GOPS for membrane formation in proton-exchange membrane fuel cells and direct methanol fuel cells (Park et al., 2001). It is considered an ideal candidate for this purpose due to its solubility in water and ability to form films. Additionally, GOPS has been studied and used as coating material on metal surfaces to increase mechanical properties (Wong et al., 2005). Liu et al. (2002) measured coating formation using 0.25% GOPS, and observed formation of approximately eight molecular layers. GOPS has also been applied for “soft chemistry”, a method to synthesize inorganic and organic material under low temperature (room temperature) (Schmidt, 1994) GOPS is also highly chemically stable to acids and free radicals (Schmidt, 1986, Maskos et al., 1992). These properties render it a preferable candidate as an additive for this

research; it polymerizes easily in acidic solution at room temperature and is able to form multilayer coating coatings (Schmidt, 1985, Maskos et al.,1992). When added to acidic solution, GOPS is able to exchange its methoxy substituents for hydroxyl groups, forming methanol and silanol in the process. This proceeds by the S_N^2 reaction mechanism shown in **Figure 12** (Liu et al., 2002, Wong et al.,2005).

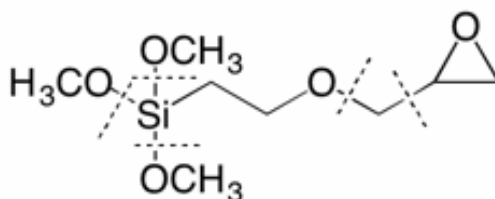


Figure 12 Structure of GOPS

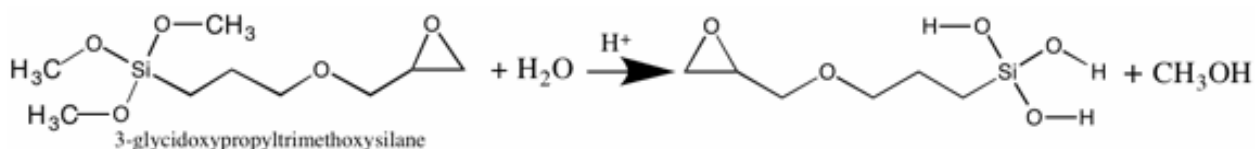


Figure 13 Hydrolysis of GOPS (Schmidt, 1994)

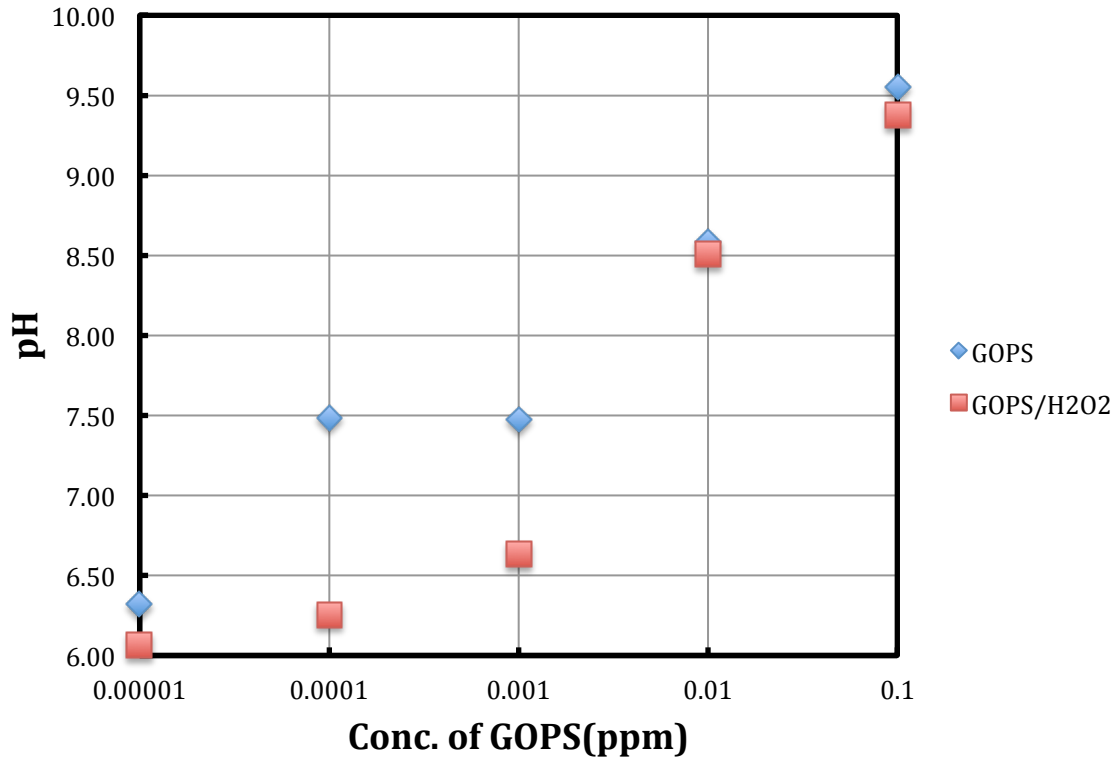


Figure 14 Effect of [GOPS] on pH

This hydrolysis reaction causes pH to increase as GOPS is added, as shown in blue in **Figure 14**. While an increase in pH from acidic to neutral is desirable, increasing to alkaline pH is undesirable. Low pH favors the growth of acidophilic bacteria. These bacteria accelerate the rate-limiting step of conversion from Fe^{2+} to Fe^{3+} , increasing formation of AMD. At pH values of about 6 and above, bacterial growth is disfavored and bacterial activity is thought to become insignificant relative to abiotic reaction rates, as mentioned in Chapter 1. While the traditional application of limestone for pH control would increase the pH to just 6.0–7.5, GOPS may increase the pH up to about 10.

In addition to treatment with Flowback water and GOPS, treatment with Flowback water, GOPS, and H_2O_2 was tested. Addition of 0.142 mg/L H_2O_2 solution reduced the increase in pH brought on by GOPS, as shown in **Figure 14**. When the concentrations of GOPS were below

0.01ppm, the differences of pH between the system with/without H₂O₂ was significant, while these differences were minor for GOPS concentrations above 0.01ppm.

The obvious differences in pH when GOPS's concentrations were below 0.01ppm may be explained by the following reaction:



The product oxygen may attack the mine rock surface that is not covered by the deposition, initiating and/or continuing pyrite oxidation and bringing down the solution's pH. Higher concentrations of GOPS are able to override this effect by inducing greater release of hydroxyl, which may react with Fe, Al, and/or other alkaline metals quickly, forming hydroxide deposition. This helps the surface to become covered with layers of coating and prevent from the oxidation attack by H₂O₂ and/or Feton reagent.

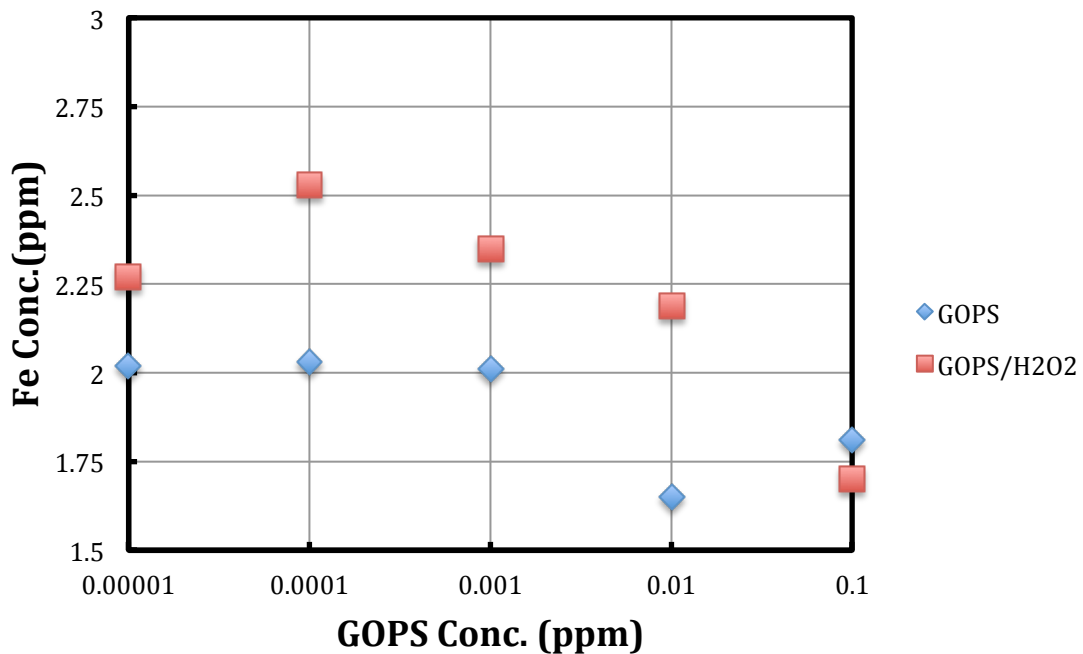


Figure 15 Effect of GOPS Treatment on [Fe]

While H_2O_2 was able to partially counteract the pH increase brought on by GOPS, solutions containing both GOPS and H_2O_2 tended to have higher concentrations of iron than those containing GOPS alone. Due to the initial oxidation of pyrite, Fe^{2+} would be available in the solution, which may react with H_2O_2 to yield the following reaction (Schmidt, 1985):

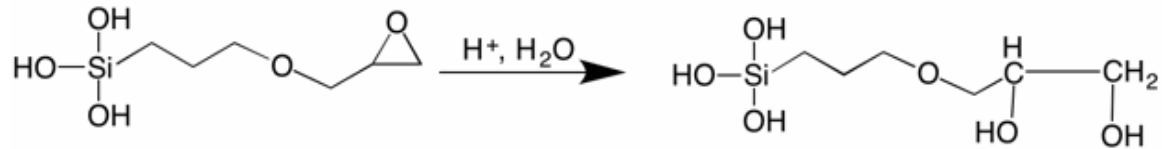


Figure 16 Reaction of GOPS (Schmidt, 1985)

This reaction opens the epoxide ring, producing the hydrophilic $-\text{OH}$. The resulting product is more hydrophilic.

In Figure 14, it can be seen that a lower concentration of iron was detected with higher concentration of GOPS for both types of solutions (with/with H_2O_2). Higher pH due to the higher concentration of GOPS is favorable for the deposition of ferric, which may be removed from the liquid phase. Additionally, higher concentrations of GOPS may encourage the crosslinking and polymerization of particles, as shown in **Figure 17 and 18**.

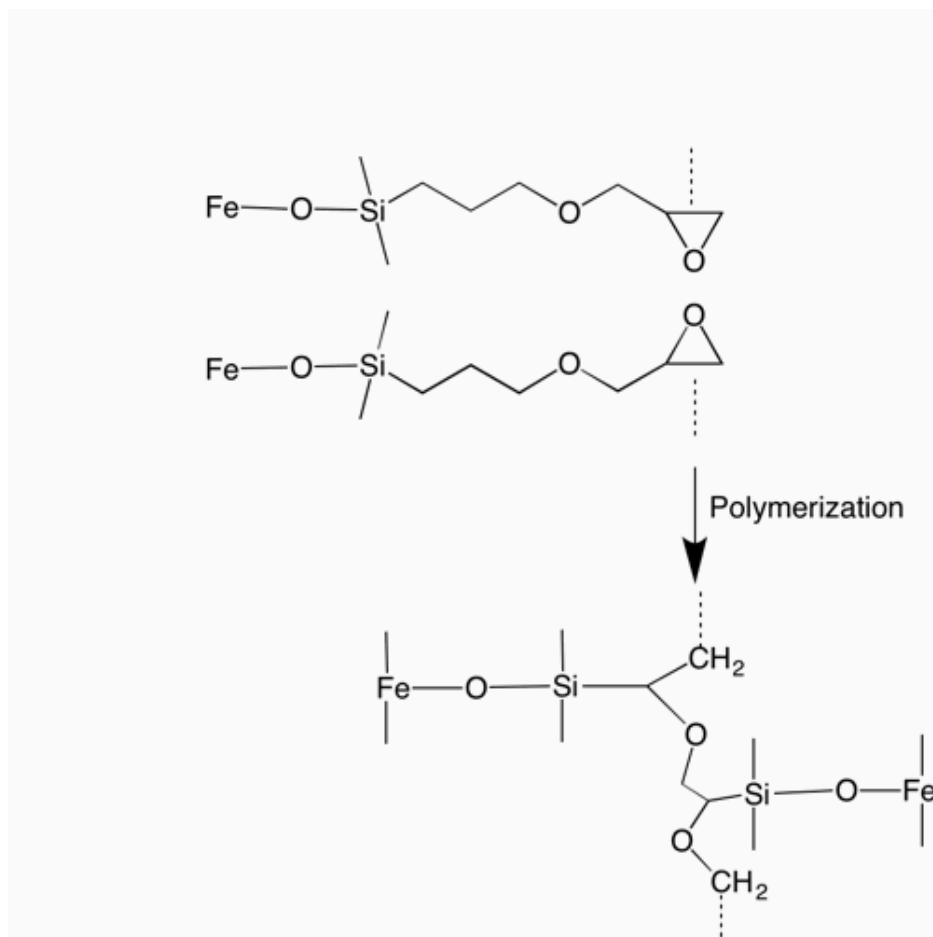


Figure 17 Crosslinking/Polymerization of GOPS (Schmidt 1985;1986)

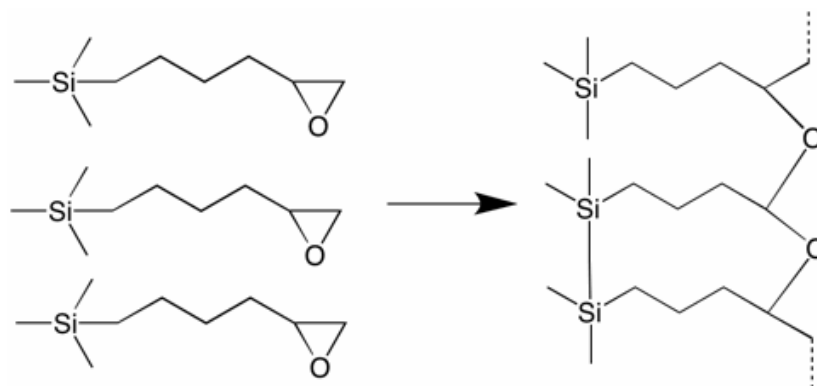


Figure 18 General Polymerization with of GOPSs (Schmidt, 1994)

GOPS is also an organic network former. It is prone to react with Fe, Al, and Mg (Schmidt, 1994, Maskos et al., 1992, Park et al., 2001) on one end, which usually are in the form of hydroxide precipitates on the mine residue surface due to the alkaline pH. The crosslinking and condensation of different solid particles reduces the surface available for dissolved oxygen and ferric iron in the solution to oxidize metal disulfides. Polymerization of GOPS bound to the mine residue surface may result in the hydrophobic tail being positioned on the particle surface. It is well documented that H₂O is an indispensable oxidant for the pyrite oxidation cycle. In Elsetinow's investigations (2003), lipids were used to suppress the pyrite oxidation for its ability to build bilayers of hydrophobic layers around the particle surface, which has achieved significant efficiency in stopping pH decrease and release of dissolved metals. In this research, the polymerization of GOPS and its bonded surface would induce multiple hydrophobic layers, building a GOPS barrier around the particle.

As shown in **Figure 18**, the lowest Fe concentration (1.61 mg/L) was measured in the sample containing 0.01 ppm GOPS. However, iron concentration increased slightly to 1.80 mg/L when the concentration of GOPS was increased from 0.01 ppm to 0.1 ppm. Also, when concentration of GOPS was 0.1 ppm, the pH was as high as 9.56, while the pH of solution having 0.01 ppm GOPS was just 8.59. As long as the pH of the solution is above 6, the formation of various iron hydroxides is favored. For pyrite, the pH point of zero charge (PZC_{pH}) is around 1, the mine residue shows strong attraction to the cations (Evangelou, 1995 (B)). As a result, the species with positive charges are more favorable to deposit on this negatively charged surface than the negatively charged species, such as Fe(OH)⁴⁺ in this case. This is not beneficial for the crosslinking and polymerization of GOPS with Fe and Al, because the bonds with Fe and Al would all be occupied by hydroxyl groups, making it difficult for GOPS to bind with them on the

surface. Additionally, higher pH means higher concentrations of hydroxyl in the solution, increasing the chance for the OH^- to react with GOPS in the weak bond as shown in the structure. The $-\text{OH}$ bond is hydrophilic, which is not helpful for suppression of oxidation.

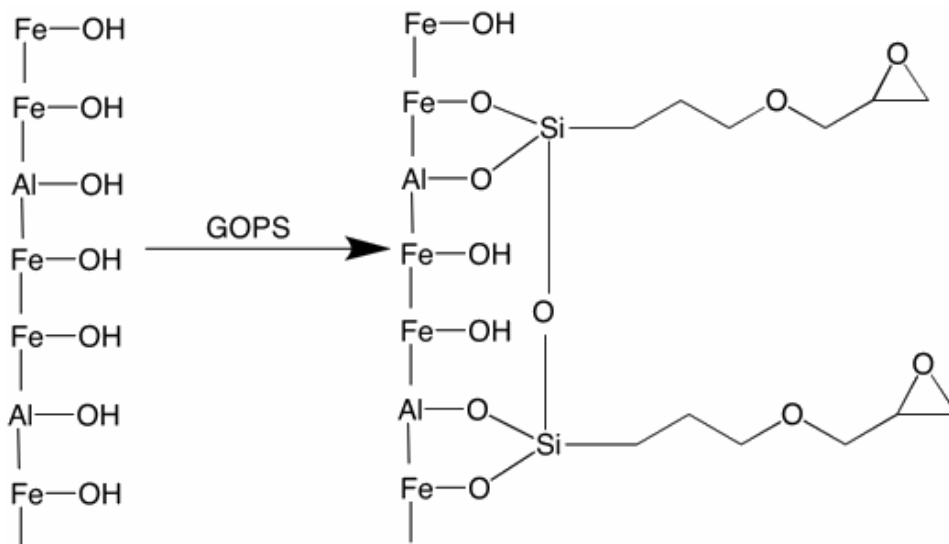


Figure 19 Crosslinking of GOPS with Fe Hydroxide and Al Hydroxide

The crosslinking and polymerization on the particle surface on the sites of Fe (oxy)hydroxides and Al hydroxides are beneficial for the solid-liquid separation because they help to form a solid and complex mesh on these particle surfaces. Mayhugh et al. have reported that at pH values lower than 4 and higher than 9, iron or aluminum concentrations in aqueous phase begin to rise (Mayhugh et al., 2005). This can be explained by the fact that Fe may complex with OH^- , forming $\text{Fe}(\text{OH})_4^-$, which dissolves in aqueous phase. This can explain why the concentration of Fe in solution derived from adding 0.1 mol/L of GOPS with pH above 9 (9.56) yields a higher concentration of Fe.

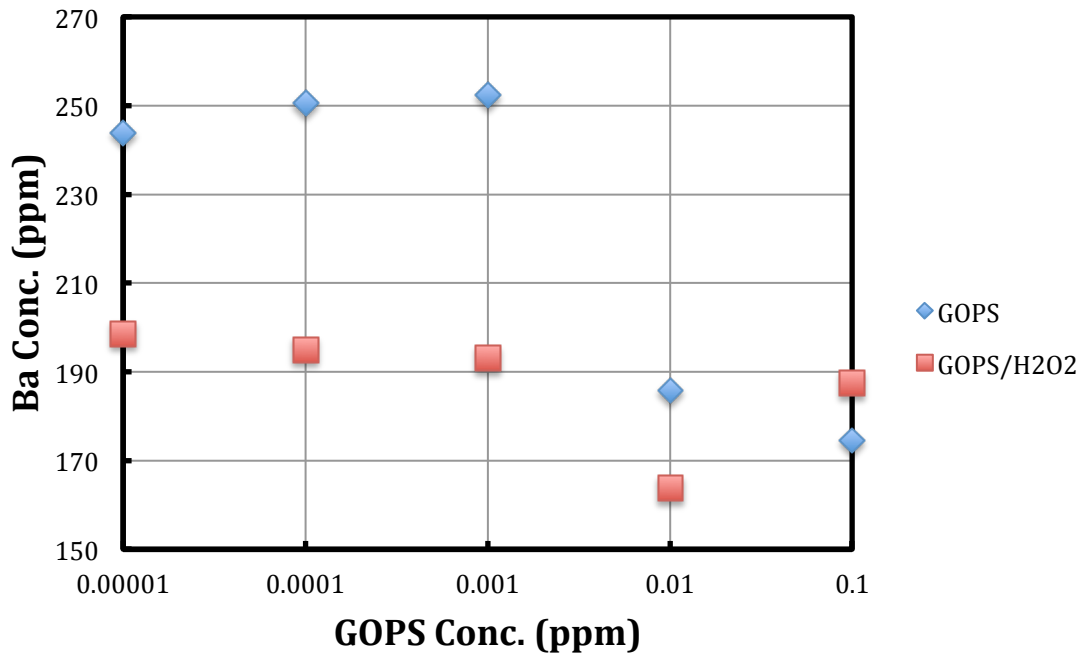


Figure 20 Effect of GOPS Treatment on [Ba]

The solutions containing GOPS alone all showed higher concentrations of Ba in solution than those with the same concentrations of GOPS with H₂O₂. It is believed that this is related to the concentration of SO₄²⁻ available in solution. The H₂O₂ is a strong oxidant that would promote the release of Fe³⁺ and its precipitates. However, at the same time, SO₄²⁻ is also the product of pyrite oxidation. Consequently, more SO₄²⁻ would be released due to the accelerating initial oxidation stage. Normally, the concentration of Ba in the flowback water is the same, more SO₄²⁻ available in the solution yields less Ba in the final samples. The extremely high concentration of Ba in solution renders the solution supersaturated in BaSO₄. Ion chromatography (IC) showed no SO₄²⁻ peak for all samples listed above. This means that they are all consumed by precipitation with barium. This is further verified by adding 100 mg/L BaCl into the sample, which did not show precipitation as would be expected if SO₄²⁻ were present.

On the other hand, for both types of solutions (with and without H₂O₂), when the concentration of GOPS added were below 0.01 ppm, the concentration of Ba in the solution was nearly constant. A significant drop (from 250 to about 190 mg/L) was observed when concentration of GOPS reached 0.01 ppm. This aligns with the result of Fe measurement, where the lowest concentration of Fe was detected in the solution containing 0.01 ppm of GOPS. For Ba, the major influence of GOPS is its effect on pH. It is well recognized that the rate of conversion from Fe²⁺ to Fe³⁺ increases as pH increases (Egiebor, 2007, Evangelou, 1995(B)), which means more SO₄²⁻ would be released as the product of faster pyrite oxidation. According to the study of Moses et al.(1991), the turnover rate of Fe (from Fe²⁺ to Fe³⁺) through O₂ exhibits a half life of only a few minutes at pH greater than 6. The concentration of Ba is still closely related to the release of SO₄²⁻. It can be verified by the fact that, in the solution containing 0.1 ppm GOPS, and the resultant pH was almost 10; pyrite oxidation was fast enough to release more sulfate within the same reaction period and induce more BaSO₄ precipitation in the solution.

Ideally, the precipitation of Fe (oxy)hydroxides would occur in the reacting samples initially, acting as the seed for the precipitation of BaSO₄. The crosslinking and polymerization of GOPS with Fe (oxy)hydroxides and Al hydroxides may act as a mesh, burying BaSO₄ in the coating layers.

4.3 CONTINUOUS COLUMN STUDIES

In this section are described the large-scale continuous-flow column tests. The results described in Chapter 3 were used to design the larger-scale column. For these tests, 500 g of mine rock was treated with 15 L of day 1 flowback water in the test column, while 500 g of mine rock was

treated with 15 L of deionized water in the control column. The test column was run for 30 days, while the control column was run for 15 days. From each column iron (Fe), barium (Ba), sulfate (SO_4^{2-}), and pH were measured daily. Additionally, aluminum (Al) and manganese (Mn) were measured.

4.3.1 pH

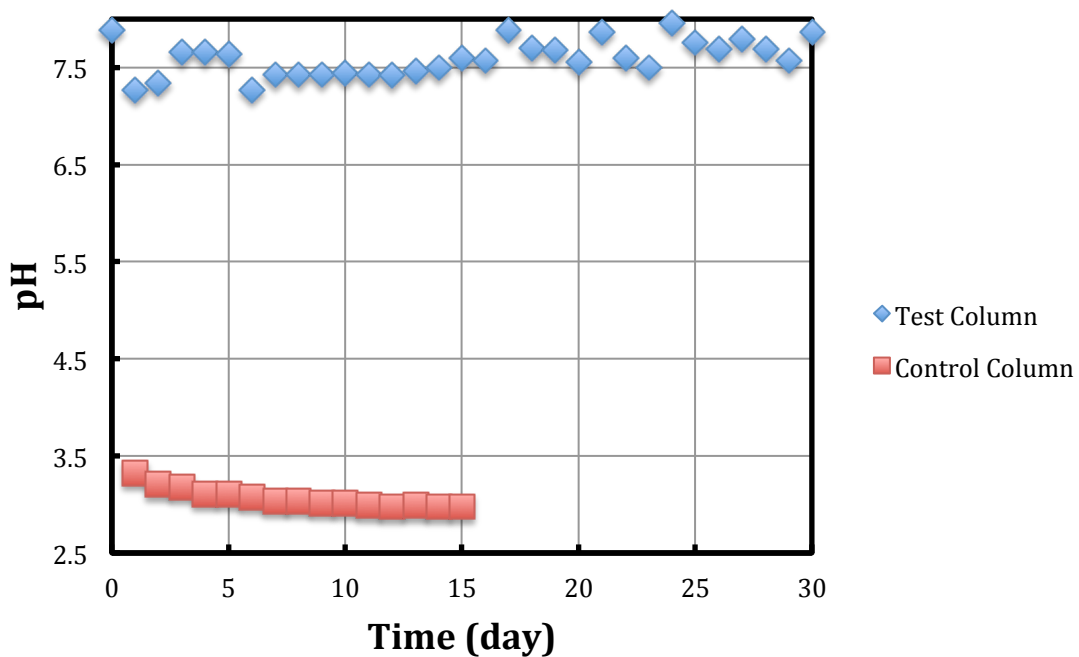


Figure 21 Control Column pH in Control Column & Test Column

From **Figure 21**, it is clear that the treatment managed to maintain the pH to around 7.5 over the 30 days of running, while in the control column, the pH kept dropping from around 3.33 to about 2.7 until Day 15. This significant difference favored the fact that in the test column, pyrite oxidation was controlled through microencapsulation. With the alkalinity provided by the flowback water and GOPS added, the pH in the test column was stably above 7, beyond the

EPA's requirement of 6.5 for treating AMD. After starting the column, the pH of the flowback water solution dropped from 7.5 from its initial value of 7.98. This was due to the initial small portion of pyrite oxidation. Over the subsequent 30 days of testing, pH stayed stable about 7.5, favoring the formation of hydroxides and oxides of various metals. To conclude, the flowback water with 0.0001 M GOPS stabilized the pH of the mine residue relative to the control.

4.3.2 Al

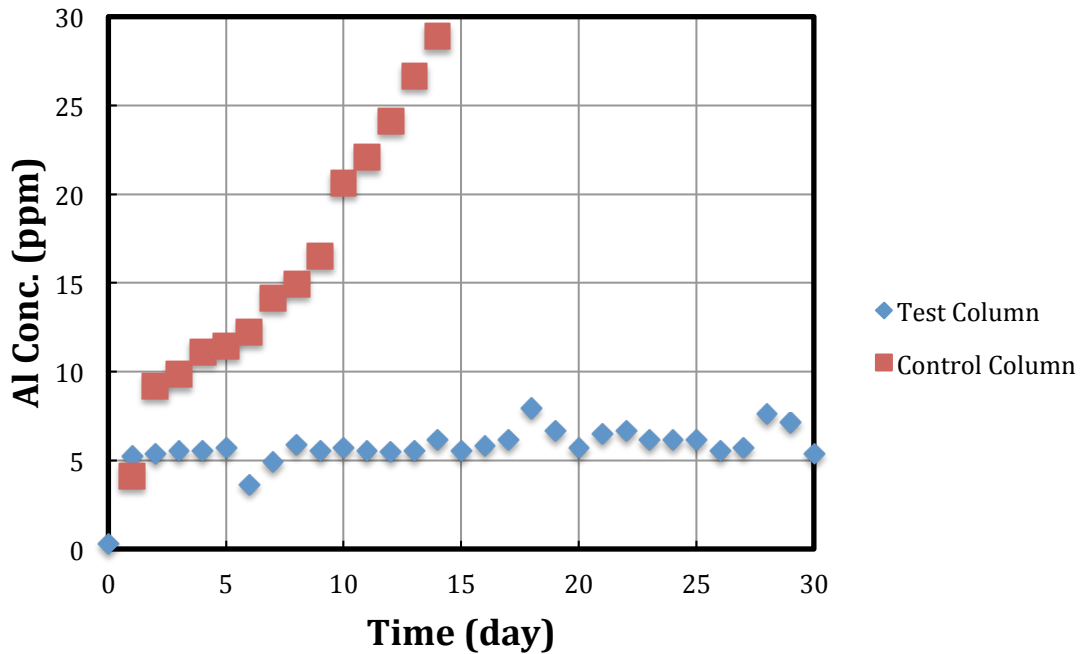


Figure 22 Concentration of Al in Control Column & Test Column

In contrast to the control column, where Al concentration increased at a first order rate, a stable state was reached for Al in the treated column. The increasing Al concentrations in the control column can be supported by the following explanations: First of all, the dissolution of Al – bearing rocks would begin when the pH was between 3 and 1, which is the case for most of the

duration (Shaw et al. 2009). Secondly, the ion exchange between Al and other metals in the bulk, especially Fe. On the other hand, it has been concluded by Li et al. (2006) that the ion exchange of Al is faster than mineral dissolution. This means that, more Fe in solution favors the release of Al, due to the ongoing exchange of Fe and Al. Consequently, Al continued to dissolve and be exchanged from the edge of surface continuously. Fe was not the only cation that kept the ion exchange of Al active. Na^+ and K^+ have also been found to be favorable to be exchanged with Al in other studies when pH ranged between 2 and 3 (Nordstrom, 1996). Also, as long as the pH stays under 4, Al would not be able to form hydroxides and become immobilized (Nordstrom and Ball, 1986), which is the case for this control system. Consequently, Al continued to dissolve and be exchanged from the edge of surface continuously. Before the control column was stopped after 15 days, a steady state had not yet been reached, since Al still exhibited a first order reaction rate. In Pennsylvania the concentrations of Al in AMD range from 1 – 108 ppm and pH ranges from 2 – 5 (Cravotta, 2008 (A),(B)). Thus, it is still possible for Al to keep increasing if the control column were run longer.

In contrast to the control column, a stable state was reached for Al in the treated column. Even there was an increase in Al, but it was quickly brought back to stable state through precipitation, encouraged by alkaline pH. Therefore, it is clear that Al was immobilized inside the mine rock through the alkaline pH and the coating formation to protect the surface.

4.3.3 Fe

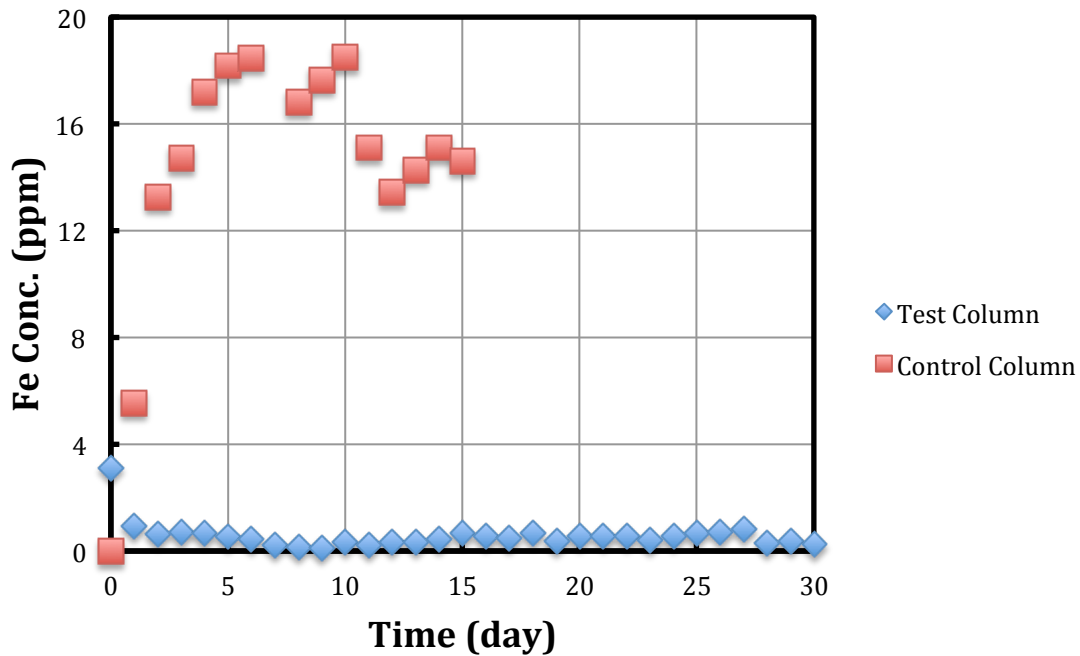


Figure 23 Concentration of Fe and Al in Control Column & Test Column

As shown in **Figure 23**, while the Fe concentrations were below 1 ppm since the start of column running, the Fe concentrations in the control column show a dramatic increase (up to 18 ppm) in the first 6 days with a decrease to around 14ppm afterwards.

For the control column, the quick release of Fe from the solid phase to the liquid phase was most likely due to pyrite oxidation. The pumping of water from the bottom of the column would enhance the pyrite oxidation for most of the particles suspended on the upward-flowing fluid, exposing more available surface for oxidants. The slight drop of Fe concentrations from 18 mg/l to 14 mg/L can be explained by the ongoing ion – exchange between Al and Fe since Day 10. As mentioned in the Chapter 1, Fe^{2+} is the product for the first step of pyrite oxidation. . In Cravotta’s investigation (2008 (A), 2008 (B)) of 140 abandoned coal mines in PA, when the pH

is between 2.6 to 7.3, ferrous ion is the major species of iron in AMD, while ferric iron is the minor species. Appelo and Postma observed that, Fe^{2+} and Al^{3+} follow this equation (1993):



The selectivity coefficient **K** is the equilibrium constant for the displacement of the cation on the solid surface by an alternative cation in the liquid phase. In this case, Fe^{2+} shows more affinity for the solid surface than Al^{3+} . From day 7 to the end of the control duration, Fe experienced a steady decrease, while there was no sign for Al to stop increasing. It is reasonable to make the assumption that the ion exchange between H^+ , Fe^{2+} and Al^{3+} on the surface has been dominant since day 7. Based on the selectivity coefficient described in **Equation 4.1.3**, Al would be preferentially partitioned on the solid surface more than Fe.

In conclusion, pyrite oxidation started immediately after the column was started, giving rise to low pH and high concentration of Fe. Simultaneously, dissolution of Al from mine rock and ion exchange between Fe^{2+} and Al^{3+} took place. In the end, the exchange reactions between Fe^{2+} and Al^{3+} on the surface may be regarded as a possible link to the lower Fe concentration in the bulk after day 10. By day 15, a steady state has not yet been reached.

For the test column, about 3.2 ppm of Fe was initially present in the flowback water. The concentration of Fe fell dramatically by the first day after the column was started. After that Fe dropped until day 10, followed by a rebound of Fe from approximately 0.1 ppm to 0.5 ppm after which it flattened out after day 15. Overall, the levels of Fe were controlled to be below 1 ppm, which is a remarkable reduction compared to the results from the control column.

Because the flowback water was withdrawn from the subsurface, ferrous iron would be the dominant form of the total Fe in the flowback water before the column started. The pumping of flowback water made it possible for ferrous iron to be oxidized to ferric iron (Fe^{3+}) and form

(oxy)hydroxides when pH was above 7. Therefore, a measurable reduction in Fe was shown. Notably, pyrite oxidation was still triggered as mine rock was exposed to water and dissolved oxygen. This led to a small increase after day 1, when concentrations of Fe were increasing slightly. As pH was always above 7, it is believed that the dominant specie of Fe was Fe^{3+} , whose (oxy)hydroxides are stable. Meanwhile, the precipitates acted as the sink for the dissolved Fe from pyrite and the coatings around particle surface started to establish, interrupting the contact between pyrite and its oxidants, explaining the drop of Fe from day 3 to day 9. Between day 10 and day 15, there was a slow rise in Fe. This can be explained by the partial covering of particle surface by the precipitates. The uncovered part of the particles would be under attack by the oxidants, continuing the release of Fe from pyrite oxidation. When the rate of iron dissolution from the pyrite oxidation exceeds that of the precipitation, an increase of Fe may be observed, which may be the case for small rise from day 10 to day 15. Then it was followed by the fluctuation, with a flattening out tail. This would be the indication of a stable and solid coating around the particle surface, where no further pyrite oxidation was occurring. At least, no trend of increasing in Fe has been noticed, justifying that no more considerable pyrite was oxidized. Nevertheless, it is possible that, only part of the particle surface has been covered by the hydrophobic coating, and a balance has been achieved between the Fe released by part of the surface being oxidized and the Fe precipitated out on the surface by favorable pH. Another important factor to be taken into consideration is that, the neutral pH (>7) can actually yield faster pyrite oxidation.

In conclusion, only a small portion of pyrite was oxidized to form the precipitates on the surface and it is beneficial for the coating formation. A relatively stable state was reached with

Fe maintained below 0.7 ppm. Overall, the levels of Fe were controlled to be below 1 ppm, which is a remarkable reduction compared to the results from the control column.

4.3.4 Sulfate

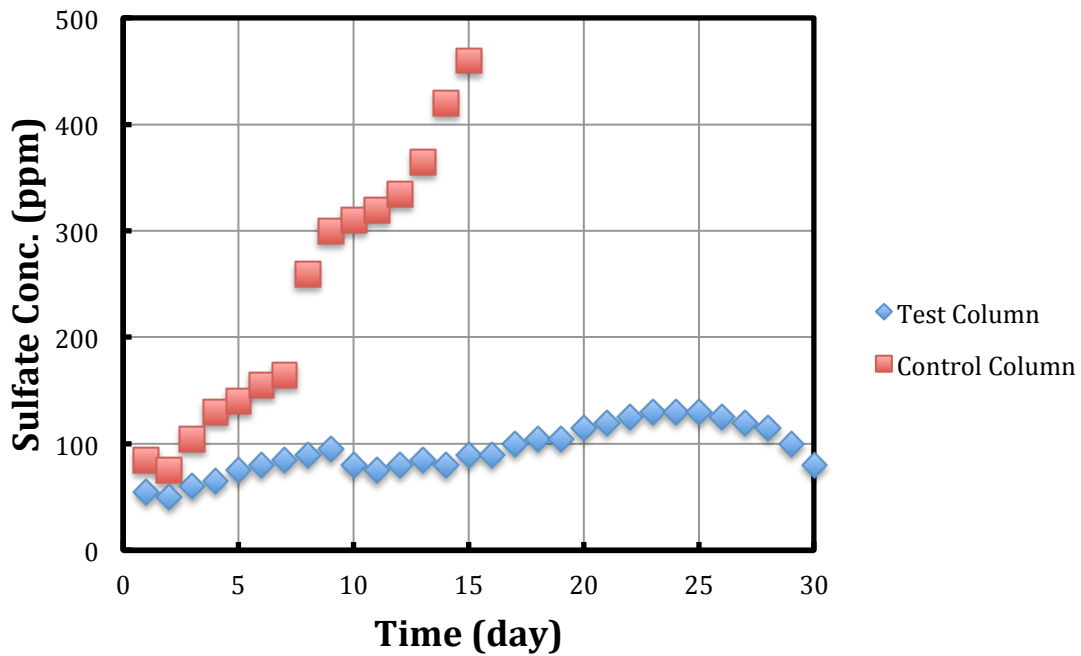


Figure 24 Sulfate Concentration. in Control Column and Test Column

Like Al, a unstoping increase of sulfate was observed in the control column. In contrast, though with variation, the levels of sulfate concentrations throughout the whole running period managed to stay way below the concentrations measured in the control column. It is true that overall, the sulfate exhibited increment over time, but when compared to the control column, the highest sulfate levels was just a third of the highest level in the control column. To some extent, the perceptible down turn of sulfate suggested that pyrite oxidation may be completely curbed.

According to the chemical equations of pyrite oxidation, 6 moles of sulfate should be produced when 1 mole of pyrite is oxidized. In control column, the levels of sulfate rose continuously due to the continuously ongoing pyrite oxidation. Sulfate's complexes with Al and Fe are soluble, giving it no alternative to escape from the liquid phase. As can be seen from the line shown, the rate of sulfate production is steady, meaning the pyrite oxidation may be the only contributor to its appearance in solution. However, Al can be coupled with sulfate to form complexes, which would be predominant, when pH is low and sulfate concentration is high (Driscoll and Postek, 1996).

In the test column, more SO_4^{2-} was introduced to the bulk solution due to pyrite oxidation. Thus, as long as pyrite oxidation continued, SO_4^{2-} continued to accumulate. As the concentration of Fe decreased on day 10, the concentration of SO_4^{2-} decreased as well. After day 10, the rate of sulfate release was slower than that during days 1 to 9. This is consistent with the hypothesis that, the part of precipitates formed on the surface were taking effect on shutting down the contact from oxidants. This can also be correlated to the pattern of Fe. As **Equations 4.3.2.1 and 4.3.2.2** indicate, as Fe dropped the ongoing pyrite oxidation would drop as well. After day 24, the pattern manifested a distinct decrease, suggesting a slow in the pyrite oxidation and the continuous reaction between Ba and SO_4^{2-} . This can also be correlated to the pattern of Fe. Then when the pyrite oxidation came to a complete stop, the sulfate produced by the initial pyrite oxidation would be consumed by Ba from the flowback water.

4.3.5 Mn

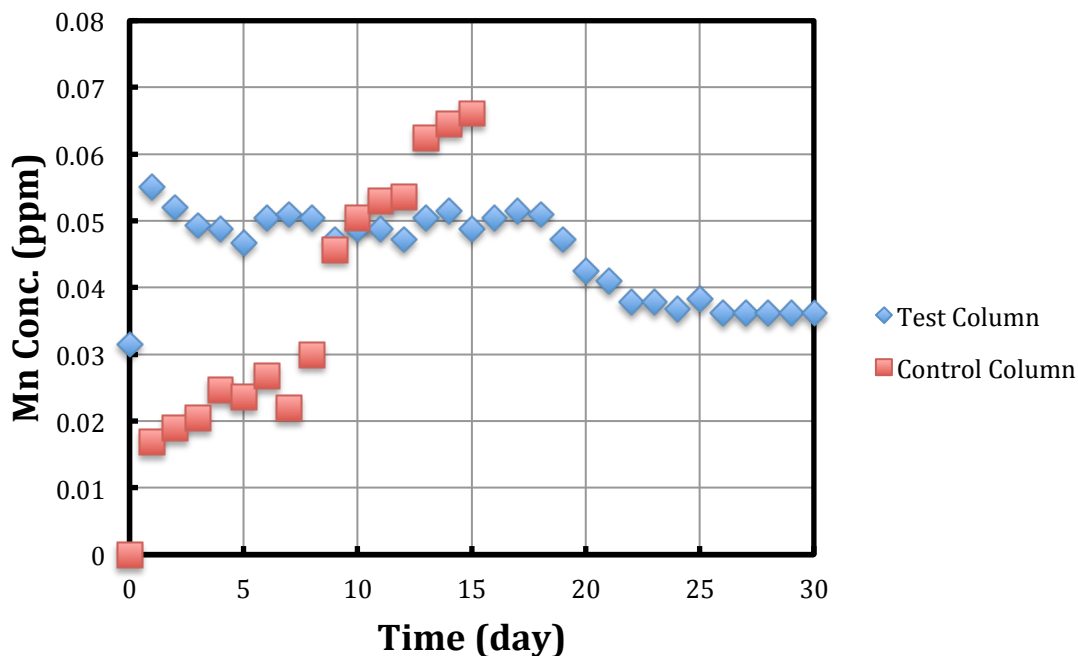


Figure 25 Concentraion of Mn in Control Column & Test Column

The concentrations of Mn in the control column did not exceed those in the test column until Day 10. However, Mn in the test column exhibited a dropping trend, and stayed constant at 0.035 ppm since Day 21 to Day 30. In contrast, consistent with the results for Al and Sulfate, Mn exhibited an overall first-order rate of dissolution. This is also promoted by the acidic pH. First of all, there was around 0.03 ppm of Mn from the flowback water, even before the running of test column. There was a slight increment of Mn concentrations when the test column started running, from 0.03 to 0.055 ppm, with no immediately following decrease. In order to remove Mn from the system, the pH in the system needs to be at least 8. It is well recognized that the

removal of Mn requires the pH of solution to be above 8, which favors the oxidation of Mn(II) to Mn(IV) and its further precipitation as Mn(OH)₂ (Hallberg and Johnson, 2005). The low oxidation of Mn(II) in solutions below pH 8 is due to the relatively slow kinetics for manganese oxidation to that of ferrous iron, even though the Mn(IV) may be precipitated out readily (Nairn and Hedin, 1993; Hallberg and Johnson, 2005). However, in the test column, the pH never reached above 8. This explains the fact that no noticeable drop of Mn concentrations was detected. The initial pyrite oxidation in the test column would favor the release of Mn from the mine rock. However, the Mn concentrations in the test column were stable. There was even a reduction from 0.05 to 0.038 ppm since Day 16. This may be attributed to the coprecipitation of Mn with other metal hydroxides in this complex chemical system. At the same time, as a more complete and stable coating layers formed on the mine surface gradually, little or even no Mn can be released from the mine rock. As a result, compared to the control column, the test column has done a relatively effective job in the curbing of further Mn release.

5.0 SUMMARY AND CONCLUSIONS

5.1 PRELIMINARY EXPERIMENTS

Preliminary batch experiments were conducted to determine the optimal dosage of flowback water, H_2O_2 , and GOPS with which to treat mine residue in order to prevent acid mine drainage through passivation of the mine residue surface. For these tests 500 mg of mine residue was treated with different volumes of each additive, with flowback water tested prior to the other two additives. The mass recovered in the liquid phase of major contaminants such as Fe, Ba, and SO_4^{2-} was used as criteria to determine the optimal dosage to be used in the subsequent column tests. Based on the results from the preliminary batch experiments, the following conclusions were drawn:

1. Through the comparison of results from different reaction times, it can be concluded that homogenous mixing may be achieved by magnetic stirring in a beaker for 30 minutes, followed by 30 minutes of settling time.
2. For 500 mg of mine rock particles of size less than 53 μm , the concerned contaminants including Fe, Ba, SO_4^{2-} , and pH, reached their lowest levels when treated with 55 mL of flowback water.
3. When various concentrations of H_2O_2 were applied as additives with the goal of maximizing available Fe^{3+} in solution for precipitation, the smallest dosage of 0.142

mg/L was ideal, as measured by the concentration of concerned elements in the bulk after reaction. Beyond that dosage, higher levels of contaminants were observed. This indicates that pyrite oxidation should not be encouraged in the initial stage.

4. When various concentrations of GOPS were applied as additives with the goal of supporting hydrophobic coating formation through complexation with Al and Fe, a dosage of 0.0001 M GOPS was ideal as measured by low levels of Fe, Ba, and SO_4^{2-} , and pH within acceptable limits. Higher concentration of GOPS lead to higher pH, but this also favors more rapid pyrite oxidation, an undesired effect.
5. When various concentrations of GOPS were applied as additives alongside 0.142 mg/L H_2O_2 , 0.1 ppm GOPS was ideal as measured by concentration of Fe, Ba, and SO_4^{2-} . This dosage is unfortunately too large to be practical.
6. Among the three tested additive combinations of H_2O_2 , GOPS, and GOPS/ H_2O_2 , 0.0001 ppm GOPS yielded the optimal result.

Based on the results listed above, the dosages of various chemicals that favor least release of pollutants have determined. A ratio of 500 mg of mine waste to 55 mL of flowback water was used to facilitate more precipitations depositing on the mine rock surface. Additionally, 0.0001 ppm GOPS was used for 500 mg of mine waste in 55 mL of flowback water to induce the formation of a hydrophobic outer coating layer. These protocol was chosen for the subsequent column tests.

5.2 COLUMN EXPERIMENTS

Larger-scale continuous-flow column tests were conducted to test the effectiveness of flowback water and GOPS at preventing acid mine drainage. A test and control column were each configured with 500 g of mine residue. The test column was treated with 5.5 L flowback water for 30 days, while the test column was treated with deionized water for 15 days. For each column the pH and concentrations of Fe, SO_4^{2-} , Mn, and Al were measured each day. Based on the results from the continuous-flow column experiments, the following conclusions were drawn:

1. Within the 15-day experiment duration for the control column a steady state had not yet been reached, as Al, Mn and SO_4^{2-} continued to rise at a first order rate.
2. Pyrite oxidation began the moment the control column was started. All metals in the control column showed a rapid and steep rise in the concentration within the first day. The fast release of metals from minerals is attributed by their dissolution under acidic pH, which was as low as 3.
3. There was a relationship between Fe and Al, which may be due to the higher affinity of ferrous ion to the solid surface than Al. Under acidic pH, ferrous iron is the predominant specie of Fe in the solution. This ion exchange reaction between Al^{3+} and Fe^{2+} may be able to explain the continuous increase of Al with a slow fall in Fe concentration by the last few days of testing.
4. In contrast to the control column, the test column rapidly reached favorable pH and stable low concentration of Fe, Al, and Mn, indicating that pyrite oxidation has been effectively curbed. When the treated column was stopped after 30 days, it appeared that a steady state had been reached within the column for these three metals. Sulfate, in contrast, varied over a relatively wide range, though it rapidly decreased over the last several days

of testing. Compared to the elevated concentrations of these elements in the control column, it is reasonable to believe the establishment of coating layers served the intended effect to prevent the further formation of AMD.

Therefore, it can be concluded from the results mentioned above that the treatment of AMD through addition of flowback water and GOPS have helped to inhibit the release of major pollutants, such as acidity, Fe, Ba, and SO_4^{2-} . More importantly, the analysis and observations from this work imply an effective establishment of the coating layers over the mine rock surface, which is the main purpose of this work to prevent the further formation AMD through microencapsulation. However, there is still a lot to be done before this technique ready for application in industry. The limitations of this work include the presence of other metals in the leachate, such as Mn, that violate the current regulation standards. Moreover, the level of total dissolved solids (TDS), which may be extremely high due to the added flowback water, was not measured in this work, but is strictly regulated by the EPA.

Application of this technique in the real world would involves costs including the transportation and storage of flowback water and GOPS reagent, as well as labor to handle the application and monitor the treatment effectiveness. According to a report of Gurtright & Giglio (2012), operators expect to pay around \$0.024 per gallon for water transport, assuming a one-hour trip by truck to move the water from its source to the operation site. The cost to store flowback water is \$0.012 - \$0.024 per gallon, while the cost of water impoundment is \$0.0024 per gallon. In this case, the cost to transport, store, and impound 1 gallon of flowback water in the mining site is \$0.03624 - \$0.04824. In reference, the cost to treat and store 1 gallon of flowback water is \$0.11 - \$0.21 and the cost to treat 1 gallon of AMD is \$0.095 - \$0.19 (Curtright & Giglio, 2012). Based on these figures, this technique is obviously less costly.

6.0 FUTURE RESEARCH

6.1 SUGGESTIONS ON FURTHER RESEARCH ON THIS WORK

This work has developed a preliminary protocol for the passive treatment of acid mine drainage using a combination of flowback water and GOPS. However, it suffers from several limitations that could be addressed through future work. This work was conducted on mine waste only from a single site, and the appropriate treatment may vary between sites; future work might compare results from multiple sites. Additionally, this work focuses on the application itself, rather than the details of how it works. Better understanding of the microscopic mechanism of action could be a helpful objective of future research, possibly leading to insight useful for improving the treatment.

In this work, only the pH and concentrations of only Fe, Al, Ba, Mn, and SO_4^{2-} were measured. However, other techniques such as scanning electron microscopy (SEM) and X-ray diffraction (XRD) could be used to obtain a higher-resolution view of the system. XRD could be used to measure the effectiveness of coating formation, quantifying what proportion of the mine residue surface has been covered. SEM could provide information about the particle shape, size, growth, and composition. These methods might also support or refute the theoretical explanations provided for some of the observations made in this work.

Also, due to the fact that flowback water itself is a waste product with extremely high levels of TDS, up to thousands of ppm, the fates and concentrations of more elements such as Sr and Mn, could be researched in greater detail. Other pollutants regulated by environmental protection agency (EPA) could be measured, and would be necessary to determine whether this technique may be actually used to comply with environmental laws. Coprecipitation of other metals with ferric (oxy)hydroxides and BaSO₄, could be measured. Other measurements such as conductivity may further clarify the processes taking place.

Additional experiments (SEM, XRD, and measurements of other minor heavy metals) could be complemented by better simulating field conditions, such as by addition of low pH water (e.g. less than 5.0) to the column periodically to simulate the effects of rainfall. Replicates (more than 2) should be done for the column experiments to ensure the results are repeatable. Finally the duration of the column test was just 1 month, while it may take up to 15 months for the mine residue toxicity (oxyanion and metals) to be flushed from the solid phase (Shokes et al., 1999). Extending this experiment to this length would make the results more informative about long – term performance of this technique.

6.2 APPLICATIONS

This work has been conducted at the laboratory–scale, and much more must be considered before it could be applied at real-world mining sites. The EPA heavily regulates discharge from active mining sites, however, the results from this work did not meet the regulations for all tested metals, and other regulated metals were not tested. However, this technique might be easier to apply to abandoned mine sites, which have less stringent and more flexible regulations.

The discharges from different mine sites vary based on geological conditions. For mines surrounded by abundant limestone, the discharge may be of neutral pH. However, in our case, the mine rock from Mather Mine (Mather, PA) was acidic. The results, including the dosage of flowback water and GOPS, are site-specific. This per-site variation is one condition that must be considered when the results are applied, and it may be appropriate to develop a controlled laboratory-scale protocol similar to the work done here for determining the appropriate levels of flowback water and GOPS for each site.

Additionally, applying the levels of flowback water and GOPS determined in this work to real-world sites would entail transportation of huge amounts of materials. When the chosen ration of 55 mL of flowback water per 500 mg of mine rock is scaled up for 1 ton of mine rock, 110,000 L of flowback water are required. The transportation of flowback water from the gas drilling site to the mine tailings site and the labor to apply these tons of flowback water on top of the mine may be too demanding to make this technique practical and realistic. As a result, improvement in the protocol may be necessary to reduce the ratio between mine waste and flowback water to a more easily-applied level. It is possible that a less than optimal volume of flowback water may be combined with additional additives, chemicals or bacteria to obtain a balance between effectiveness and feasibility of treatment.

Another limitation of this work that would influence its real application is that the column tests had complete contact between the flowback water and mine residue for 30 days. In real-world application, flowback water with additive(s) would be poured on top of mine tailings, and it may just take less than 1 day for the liquid to flow from the top of mining piles to the bottom. This short contact time may not be enough for the coating layers to form. However, if a continuous-flow system were used to recycle the flowback water as it trickled through the mine

rock, the surface would be surrounded by the treating liquid for a longer time, facilitating the formation of coating layers on the surface of mine rock.

To conclude, the work presented here is an initial investigation of how the passive technique of microencapsulation through application of flowback water and GOPS may be an alternative for the treatment and prevention AMD. Much further work is necessary before the technique may be used in real-world industrial applications.

BIBLIOGRAPHY

Appelo, C.A.J. and Postma, D. (1993). *Geochemistry, groundwater and pollution*. A. A. Balkema Publishers. Amsterdam, The Netherlands.

Brown, A. D.; Jurinak, J. J., Mechanism of pyrite oxidation in aqueous mixtures. *J. Environ. Qual.* 1989, 18, 545.

Benner, S. G., D. W. Blowes, W. D. Gould, R. B. Herbert,, and C. J. Ptacek. "Geochemistry of a Permeable Reactive Barrier for Metals and Acid Mine Drainage." *Environmental Science & Technology* 33.16 (1999): 2793-799. Print.

Caruccio, F. T., J.C. Ferm, J. Horne, G. Geidel, B. Bagenz, Paleoenvironment of Coal and Its Relation to Drainage Quality. Agency, U. S. E. P., Ed. Cincinnati, Ohio, 1977.

Cortina, J. L.; Lagreca, I.; De Pablo, J.; Cama, J.; Ayora, C., Passive in situ remediation of metal-polluted water with caustic magnesia: Evidence from column experiments. *Environ. Sci. Technol.* 2003, 37 (91971-1977).

Cravotta, Charles A. "Dissolved Metals and Associated Constituents in Abandoned Coal-mine Discharges, Pennsylvania, USA. Part 1: Constituent Quantities and Correlations." *Applied Geochemistry* 23.2 (2008): 166-202. Print (A).

Cravotta, Charles A. "Dissolved Metals and Associated Constituents in Abandoned Coal-mine Discharges, Pennsylvania, USA. Part 2: Geochemical Controls on Constituent Concentrations." *Applied Geochemistry* 23.2 (2008): 203-26. Print.

Caldeira, C. "Pyrite Oxidation in Alkaline Solutions: Nature of the Product Layer." *International Journal of Mineral Processing* 72.1-4 (2003): 373-86. Print.

Collins, M., Rasmuson, A., 1986. Distribution and Flow of Water in Unsaturated Layered Cover Materials for Waste Rock. National Swedish Environmental Protection Board, Report 3088.

Curtright, Aimee E., and Kate Giglio. Coal Mine Drainage for Marcellus Shale Natural Gas Extraction: Proceedings and Recommendations from a Roundtable on Feasibility and Challenges. Santa Monica, CA: Rand Corporation, 2012. Print.

Driscoll C.T., and Postek K.M. (1996). The chemistry of aluminum in surface waters. In: G. Sposito (ed.), *The Environmental Chemistry of Aluminum*. CRC Press, Boca Raton, FL. pp. 363–418 Chapter 9.

Egiebor, N. O.; Oni, B., Acid rock drainage formation and treatment: a review. *Asia- Pacific Journal of Chemical Engineering* 2007, 2, 16.

Evangelou, V. P., *Pyrite Oxidation and Its Control*. CRC Press, Inc: 1995 (A).

Evangelou, V. P., Potential of microencapsulation of pyrite by artificial inducement of FePO₄ coatings. *Environ. Qual.* 1995, 24, 8 (B).

Evangelou, V. P., Pyrite oxidation inhibition in coal waste by PO₄ and H₂O₂ pH-buffered pretreatment *J. Mining Environ* 1996, 10.

Evangelou, V. P.; Seta, A. K., Potential role of bicarbonate during pyrite oxidation. *Environ. Sci. Technol.* 1998, 32 (14), 8.

Evangelou, V. P., *Pyrite chemistry: the key for abatement of acid mine drainage*. Springer: Berlin, 1998; p 16.

Evangelou, V. P., Pyrite microencapsulation technologies: Principles and potential field application. *Ecological Engineering* 2001, 17, 14.

Elsetinowa, A. R.; Bordab, M. J.; Schoonenb, M. A. A.; Strongina, D. R., Suppression of pyrite oxidation in acidic aqueous environments using lipids having two hydrophobic tails. *Advances in Environmental Research* 2003, 7, 969-974.

Elsetinow, A. "Suppression of Pyrite Oxidation in Acidic Aqueous Environments Using Lipids Having Two Hydrophobic Tails." *Advances in Environmental Research* 7.4 (2003): 969-74.

Golab, A. N.; Peterson, M. A.; Indraratna, B., Selection of potential reactive materials for a permeable reactive barriers for remediating acidic groundwater in acid sulphate soil terrains. *Quarterly Journal of Engineering Geology and Hydrogeology* 2006, 39, 209-223.

Hoffmann, M. R.; Faust, B. C.; Panda, F. A.; Koo, H. H.; Tsuchia, H. M., Kinetics of the removal of iron pyrite from coal by microbial catalysis. *Appl. Environ. Microbiol.* 1981, 42, 259.

Hedin, R. S.; Narin, R. W.; Kleinmann, R. L. P., *Passive Treatment of Acid Mine Drainage*. Interior, U. S. D. o. T., Ed. 1993.

Huang, X.; Evangelou, V. P., Suppression of pyrite oxidation rate by phosphate addition. In *Environmental geochemistry of sulfide oxidation*, Alpers, C. N.; Blowers, D. W., Eds. ACS: Washington, D.C., 1994; pp 562-573.

Huminicki, D. M. C.; Rimstidt, J. D., Iron oxyhydroxide coating of pyrite for acid mine drainage control. *Applied Geochemistry* 2009, 24 (9), 1626-1634.

Hallberg, Kevin B., and D. Barrie Johnson. "Biological Manganese Removal from Acid Mine Drainage in Constructed Wetlands and Prototype Bioreactors." *Science of The Total Environment* 338.1-2 (2005): 115-24. Print.

Iler, R. K., *The chemistry of silica: solubility, polymerization, colloid and surface properties, and biochemistry*. John Wiley & Sons: New York, 1979.

Johnson, D. Barrie, K. B. H., Acid mine drainage remediation options: a reievew. *Siencie of the Total Environment* 2005, 338 (3), 13.

Jaynes. D.B., R., A.S. and Pionke, H.B., Acid mine drainage from reclaimed coal strip mines. 1. Model description. *Water Resour. Res.*, 1984, 20 (233-242).

J.R., C.; M., V. F.; T.N., S., Pyrite: Physical and chemical textures. *Mineralium Deposita* 1998, 34, 20.

Kleinmann, R. L. P.; Hedin, R., *In proceeding of the international symposium on tailings and effluent management*. Pergamon Press: New York, 1989.

Kargbo, D. M.; Atallah, G.; Chatterjee, S., Inhibition of Pyrite Oxidation by a phospholipid in the presence of silicate. *Environ. Sci. Technol* 2004, 38 (12), 10.

Kargbo, D. M.; Chatterjee, S., Stability of Silicate Coatings on Pyrite Surfaces in a Low pH Environment. *Journal of Environmental Engineering* 2005, 131 (9), 9

Kleiv, R. A.; Shao, L.; Sandvik, K. L.; Wu, W.; Song, C. Y., Study on Copper Adsorption on Olivine. *J. Univ. Sci. Technol.* 2001, 8 (1), 1.

Lindsay, W. L., *Chemical Equilibria in Soil*. John Wiley and Sons: New York, 1979.

Lalvani, S. B.; Weston, A.; Masden, J. T., Characteriazation of semiconducting properties of naturally occurring polycrystalline pyrite. *Journal of Materials Science* 25 (1), 107-112.

Lalvani, S. B.; Zhang, G.; Lalvani, L. S., Coal pyrite passivation due to humic acids and lignin treatment. *Fuel. Sci. Technol. Int.* 1996, 14 (9), 13.

Lapakko, K. A.; Antonson, D. A., PYRITE OXIDATION RATES FROM HUMIDITY CELL TESTING OF GREENSTONE ROCK. In *7th ICARD*, ASMR: Lexington, KY, 2006.

Lovett, R., and P. Ziemkiewicz. 1991 In *Calcium peroxide for treatment of acid mine drainage*, Second International Conference on the Abatement of Acidic Drainage. , Montreal, CAN, Montreal, CAN, 1991; pp 35-46.

Liu X, Neoh KG, Kang ET (2002) *Langmuir* 18:9041–9047

Li, J., Xu, R. Tiwari, D., and Ji, G. (2006). Mechanism of aluminum release from variable charge soils induced by low-molecular-weight organic acids: Kinetic study. *Geochim. et Cosmochim. Acta*, 70, 2755.

Moses, C. O.; Nordstrom, D. K.; Herman, J. S.; Mills, A., Aqueous pyrite oxidation by dissolved oxygen and by ferric iron. *Geochim* 1987, 54.

Moses, C. O.; Herman, J., Pyrite oxidation at circumneutral pH. *Geochim. Cosmochim. Acta* 55, 471-482.

M.A., B.; W.L., D.; M., E., Leachate Chemistry of Mixtures of Fly Ash and Alkaline Coal Refuse. In *World of Coal Ash*, Northern Kentucky, 2007.

Malmström, Maria E., Sten Berglund, and Jerker Jarsjö. "Combined Effects of Spatially Variable Flow and Mineralogy on the Attenuation of Acid Mine Drainage in Groundwater." *Applied Geochemistry* 23.6 (2008): 1419-436. Print.

McConchie, D.; Clark, M.; Davies - McConchie, F. In *New strategies for the management of bauxite refinery residue (red mud)*, 6th International Alumina Quality Workshop, Brisbane, AQW Inc.: Brisbane, 2002; pp 327-332.

Maskos Uwe, and Edwin M. Southern. "Oligonucleotide hybridisation on glass supports: a novel linker for oligonucleotide synthesis and hybridisation properties of oligonucleotides synthesised in situ." *Nucleic Acids Research* 20.7 (1992): 1679-684. Oxford University Press. Web.

Mayhugh, James, and Paul Ziemkiewicz. *Treatment of Chloride Contaminated Mine Water in NW West Virginia WVWRI Project Wri 54*. Rep. no. 2003WV16B. N.p.: n.p., 2005. Print.

Nicholson, R. V.; Gillham, R. W.; Reardon, E. J., Pyrite oxidation in carbonate-buffered solution: 2. Rate control by oxide coatings. *Geochim* 1990, (Acta 54), 8.

Nordstrom, D. K., *Aqueous pyrite oxidation and the consequent formation of secondary iron minerals*. Soil Society of Merical Press: 1982.

Nordstrom, D.K. and Ball, J. W. (1986). The geochemical behavior of aluminum in acidified surface waters. *Science*, 232, 54-58.

Nordstrom D.K., and May H.M. (1996). Aqueous equilibrium data for mononuclear aluminum species. In: Sposito G, (ed.), *The environmental chemistry of aluminum*, 2nd ed. CRC Press, Boca Raton, FL. p 39-80.

Olson, L. L., The interaction of Fe(III) with Si(OH)₄. *J. Inorg. Nucl. Chem.* 1973, 35, 1977-1985.

Orndorff, Zenah, Lee Daniels, Mike Beck, and Matt Eick. "Leaching potentials of coal spoil and refuse: acid-base interactions and electrical conductivity." *Bridging Reclamation Science and the Community*. Proc. of 2010 National Meeting of the American Society of Mining and Reclamation, Pittsburgh. Lexington: ASMR, 2010. N. pag. Print.

Parisi, D.; Horeman, J.; Rastogi, V. In *Use of bactericides to control acid mine drainage from surface operations*, International Land Reclamation and Mine Drainage Conference, Pittsburgh, PA, April 24-29, 1994; USDI, Bureau of Mines SP: Pittsburgh, PA, 1994; pp 329-325.

Pérez-López, R.; Nieto, J. M.; de Almodóvar, G. R., Immobilization of toxic elements in mine residues derived from mining activities in the Iberian Pyrite Belt (SW Spain): Laboratory experiments. *Applied Geochemistry* 2007, 22 (9), 1919-1935.

Pérez-López, R.; Cama, J.; Miguel Nieto, J.; Ayora, C.; Saaltink, M. W., Attenuation of pyrite oxidation with a fly ash pre-barrier: Reactive transport modelling of column experiments. *Applied Geochemistry* 2009, 24 (9), 1712-1723.

Park, Yong-il, and Masayuki Nagai. "Proton-Conducting Properties of Inorganic-Organic Nanocomposites Proton-Exchange Nanocomposite Membranes Based on 3-Glycidoxypropyltrimethoxysilane and Tetraethylorthosilicate." *Journal of The Electrochemical Society* 148.6 (2001): A616.

Rimstidt, J. D.; Vaughan, D. J., Pyrite oxidation: a state-of-the-art assessment of the reaction mechanism. *Geochimica et Cosmochimica Acta* 2003, 67 (5), 873-880.

Schmidt, H., and B. Seiferling. "Chemistry and Applications of Organic-Inorganic Polymers." *Mal. Res. Soc. Symp. Proc.* 73 (1986): 739-49.

Schmidt, H. "New Type of Non-crystalline Solids between Inorganic and Organic Materials." *Journal of Non-Crystalline Solids* 73.1-3 (1985): 681-91.

S, C.; R., Z., *In proceedings of the Symposium on Emerging Process Technologies for a Cleaner Environment*. SME: Phoenix, AZ, 1992.

Singer, P. C.; Stumm, W., Acidic Mine Drainage: the rate-determining step. *Science* 1970, (167), 3.

Skousen, A. R.; G. Geidel; Foreman, J.; Evans, R.; Hellier, W.; the, m. o.; Group, A. a. R. W., *Handbook of Technologies for avoidance and remediation of acid mine drainage*. The National Mine Land Reclamation Center located at West Virginia University in Morgantown, West Virginia: 1998.

Schmidt, H. "Multifunctional Inorganic-organic Composite Sol-gel Coatings for Glass Surfaces." *Journal of Non-Crystalline Solids* 178 (1994): 302-12.

Shokes, Tamara E., and Gregory Möller. "Removal of Dissolved Heavy Metals from Acid Rock Drainage Using Iron Metal." *Environmental Science & Technology* 33.2 (1999): 282-87. Print.

Shaw, Sean A., Dereck Peak, and M. Jim Hendry. "Investigation of Acidic Dissolution of Mixed Clays between PH 1.0 and -3.0 Using Si and Al X-ray Absorption near Edge Structure." *Geochimica Et Cosmochimica Acta* 73.14 (2009): 4151-165. Print.

Vaughan, D. J.; J.R., C., *Mineral Chemistry of Metal Sulfides*. Cambridge University Press: New York, 1978; p 36.

W, S.; J.J, M., *Aquatic Chemistry: An introduction Emphasizing Chemical Equalibria in Natural Waters*. Wiley: New York, 1981; p 780.

Wildeman, T.; Gusek, G.; J., B., *Wetland Design for Mining Operations*. Bitech Publ: BC, Canada, 1993.

Wentzler, T. H.; F.F., A. In *The symposium on Emerging Process Technologies for a Cleaner Environment*, Phoenix, AZ, Chander, S.; Richardson, P. E.; El - Shall, H., Eds. SME: Phoenix, AZ, 1992; p 149.

Weber, W. J.; Stumm, W., Formation of a silicato-iron(III) complex in dilute aqueous solution. *Inorg. Nucl. Chem.* 1965, 28, 237-239.

Wong, April K.Y., and Ulrich J. Krull. "Surface Characterization of 3-glycidoxypropyltrimethoxysilane Films on Silicon-based Substrates." *Anal Bioanal Chem* 383 (2005): 187-200. Print.

Wang, Jenny Weijun, Dorin Bejan, and Nigel J. Bunce. "Removal of Arsenic from Synthetic Acid Mine Drainage by Electrochemical PH Adjustment and Coprecipitation with Iron Hydroxide." *Environ. Sci. Technol.* 37.19 (2003): 4500-506. Print.

Yee N., S. S., Benning L.G., Nguyen T.H., The rate of ferrihydrite transformation to goethite via the Fe(II) pathway. *American Mineralogist* 2006, 91, 92-96.

Zhang, Y. L. E., V. P., formation of ferric hydroxide-silica coatings on pyrite and its oxidation behavior. *Soil Science* 1998, 163 (1);

Zhang, Y. L. E., V. P., Influence of iron oxide forming conditions on pyrite oxidation. *Soil Sci.* 1996, 161, 13.

Ziemkiewicz, P. F.; Skousen, J. G.; Brant, D. L., Acid mine drainage with armored limestone in open limestone channels. *Journal of Environmental Quality* 1997, 26, 8.